Characterization of the Spatiotemporal Network in Prefrontal Cortex-Hippocampal Synchronization: The Role of the Thalamic Nucleus Reuniens and Delta Band 2-5 Hz Oscillations

Abstract

Background: Schizophrenia is a devastating mental health illness in which our pharmacologic options do not treat the cognitive deficits that largely contribute to long-term disability. Problems with cognition likely arise from dysfunctional neural networks in which spatially distinct brain regions are unable to temporally coordinate electrical activity accurately. More specifically, the hippocampus (HC) normally achieves long-range, temporal coordination through generation of theta (4-8 Hz) oscillations by which the prefrontal cortex (PFC) can synchronize its activity. This synchronization occurs through direct HC-to-PFC monosynaptic projections, and disruptions in this pathway can replicate key features of schizophrenia. Although prior research has concentrated heavily on HC-to-PFC theta oscillatory synchronization, the neural network by which PFC exerts "top-down" influence back to HC is largely unknown for at least two reasons. For one, unlike direct HC-to-PFC projections, PFC-to-HC projections are indirect, mainly occurring through a synapse in the thalamic nucleus reunions (nRe). Secondly, the oscillatory band utilized by PFC to synchronize HC activity is largely unknown, although limited evidence suggests a 2-5 Hz oscillation as a potential candidate. The overall aim of this thesis was to characterize the circuitry by which PFC coordinates HC activity. We hypothesized PFC-to-HC synchronization occurs through a 2-5 Hz oscillation that is mediated through nRe.

Methods: Local field potentials (LFPs) were recorded in PFC, HC, and nRe in normal rats (n= 15) under urethane anesthesia. The nucleus reticularis pontis oralis (RPO) was stimulated at five intensity levels to induce theta oscillations in HC. LFPs during RPO stimulation were extracted and underwent fast Fourier transform. Linear regression analysis (Pearson's correlation coefficient, r) was performed to analyze the relationship between peak oscillatory frequency and power spectrum density in PFC and HC as a function of RPO stimulus intensity. Peak frequencies for theta and 2-5 Hz were identified in HC and PFC spectra, respectively, and spectral power at these frequencies were identified for each signal. Pairwise correlations were calculated between power spectrum density in PFC, HC, and nRe within the 2-5 Hz and theta bands to assess synchronization. Partial correlational analysis was performed between HC-PFC to statically remove the influence of nRe signal to characterize its role in PFC-HC synchronization. In the second set of experiments, LFPs were recorded in PFC and HC during

local lidocaine *in vivo* inactivation of nRe (n=4 rats). Coherence between HC-PFC was calculated before and after lidocaine injections to assess influence of nRe.

Results: As previously described, theta oscillations were the prominent signal in HC during RPO stimulation. In comparison, a narrow-band oscillation within the 2-5 Hz range (distinct from wide-band delta) dominated PFC signals at low RPO stimulus intensities. Oscillatory frequency increased linearly with RPO stimulus intensity for theta ($r = 0.64$, $p<0.001$) and 2-5 Hz ($r =0.37$, $p<0.01$) frequency bands. However, these two oscillations followed an opposite trend with respect to power density: theta power increased ($r = 0.63$, $p <0.001$), whereas 2-5 Hz power decreased ($r = -0.60$, $p<0.001$) with RPO stimulus intensity, suggesting a negative coupling between the two signals. PFC-HC signals were significantly correlated for both theta and 2-5 Hz oscillations in 7 out of the 15 rats (47%). For this subgroup, PFC-HC partial correlation, controlling for nRe signal, eliminated residual PFC-HC correlations for the 2-5 Hz oscillation (correlation $r=0.81$, partial correlation $r=0.13$, $p<0.001$), but had no significant effect on HC-PFC correlations for theta oscillation (correlation $r=0.65$, partial correlation $r=0.61$, $p=0.53$). PFC-HC coherence of 2-5 Hz oscillation significantly decreased after lidocaine injection (coherence pre-lidocaine 0.73, post-lidocaine 0.34, $p<0.01$), but had little effect on coherence for theta oscillation (coherence pre-lidocaine =0.52, post-lidocaine =0.48, $p=0.19$).

Discussion: Our results support that HC-PFC synchronization occurs not only by previously reported HC theta rhythm, but also by a second narrow-band oscillation in the 2-5 Hz range that dominates PFC activity. Importantly, removal of nRe influence, either statistically (using partial correlation) or experimentally (by *in vivo* lidocaine inactivation) significantly reduces PFC-HC coupling within the 2-5 Hz band, but has minimal effect on HC-PFC theta coupling, suggesting that nRe mediates PFC-HC 2-5 Hz but not theta oscillatory synchronization. In summary, this thesis proposes a novel thalamo-cortical (nRe-PFC) network by which PFC-HC synchronization occurs through a 2-5 Hz oscillation that is mediated through nRe. In contrast, reciprocal HC-to-PFC synchronization occurs through the theta band via a direct, monosynaptic projection. This network is likely dynamic by which the strength of PFC-HC coupling between theta and 2-5 Hz oscillatory bands vary depending on RPO stimulation intensity level. In the future, continued elucidation of this neural network will likely offer a deeper understanding of the cognitive dysfunction in schizophrenia, and thus the potential for improved treatment options.

Acknowledgements

I would like to thank my thesis advisor, Dr. Bernat Kocsis, for his invaluable support, guidance, and expertise throughout all aspects of this thesis work. Without his efforts, this thesis would not be possible.

I would also like to thank lab members, Frans Pettersson Svensson and Amna Mazeh, who assisted with surgical procedures, electrophysiology recordings, and histology.

Funding and Disclosures

Financial support for this work was obtained through Harvard Medical School Scholars in Medicine Office and NIH funding (PI Dr. Bernat Kocsis).

Parts of this thesis were accepted for publication in *Brain Structure and Function*.

Table of Contents

Glossary vi
Introduction 1
1. Overview of Oscillatory Networks 1
2. Impaired Neuronal Oscillations in Schizophrenia 3
3. The Prefrontal Cortex and Hippocampal Circuitry 5
4. Specific Aims 7
Methods 10
1. Animals 10
2. Surgical Procedures 10
3. Electrophysiological Recordings 10
4. Pharmacological Inactivation of the Thalamic Nucleus Reuniens 11
5. Histological Procedure 11
6. Data Analysis 11
Results 14
1. Theta and 2-5 Hz Oscillation Characterization in Urethane-Anesthetized Rats 14
2. RPO Stimulation Simultaneously Induces 2-5 Hz Oscillation in PFC and Theta Rhythm in HC 14
3. Differential Contribution of nRe to PFC-HC 2-5 Hz and Theta Coupling 16
4. The effect of nRe *in vivo* Lidocaine Inhibition on PFC-HC Coupling 18
Discussion 19
1. The Role of Theta and 2-5 Hz Oscillation in Bidirectional HC-PFC Synchronization 19
2. The Role of nRe in PFC-to-HC 2-5 Hz Synchronization 21
3. Study Limitations and Future Directions 23
Summary 25
References 27
Tables and Figures 37
Table 1. Percentage of rats (n=15) with significant power density correlations. 37
Figure 2. 2-5 Hz oscillation elicited in PFC simultaneously with HC theta by RPO stimulation. 39
Figure 3. The changes in frequency and power of 2-5 Hz and theta oscillations elicited by stimulation of RPO at five different stimulus intensities. 40
Figure 4. The relationship between PFC, HC, and nRe rhythmic LFPs at 2-5 Hz and theta oscillations. 42
Figure 5. Partialization of significant PFC-HC correlations by nRe. 43
Figure 6. Effect of nRe lidocaine inactivation on HC-PFC 2-5 Hz and theta coherence. 45
Figure 7. Possible models of HC-PFC oscillatory coupling at two frequencies. 46

Glossary

AMY: amygdala

CA1, CA3*: Cornu Ammonis* 1, 3

DG: dentate gyrus

EC: entorhinal cortex

FFT: fast Fourier transform

HC: hippocampus

- vHC: ventral hippocampus
- dHC: dorsal hippocampus

LFP: local field potentials

MS: medial septum

nRe: nucleus reuniens

PFC: prefrontal cortex

- mPFC: medial prefrontal cortex

RPO: reticularis pontis oralis

SUM: supramammillary nucleus

VTA: ventral tegmental area

Introduction

Schizophrenia is a major health problem for which no cure exists. Cognitive dysfunction, a key debilitating symptom of the disease, largely results from impaired oscillatory synchronization between HC and PFC (1). Earlier research has established the functional role of the HC theta (4-10 Hz) oscillations driving PFC synchronization, and disruption of this pathway can replicate fundamental features of schizophrenia (2, 3). In comparison, synchronization of neuronal activity from PFC-to-HC direction is less understood for at least two reasons: 1) the specific oscillatory frequency band that PFC harnesses to drive HC synchronization is unknown; and 2) unlike the direct, monosynaptic HC-to-PFC connections, projections from PFC-to-HC are indirect and multisynaptic, one of which occurs through the thalamic, nRe. We directly address these two issues by proposing an innovative functional model for PFC-to-HC synchronization that is founded on prior research efforts and the experimental evidence outlined in this thesis. More specifically, **this thesis proposes a thalamo-cortical (nRe-PFC) network that utilizes a 2-5 Hz oscillation to drive PFC-to-HC synchronization, which is mediated though nRe. Reciprocal HC theta drive enters this thalamo-cortical network primarily through a direct PFC-to-HC projection, and co-occurs with this 2-5 Hz oscillation** (See Fig. 7B). Considering that PFC is the master regulator of cognitive behavior, identifying the network involved in PFC-to-HC synchronization should provide key insight into the cognitive pathophysiology found in schizophrenia, and ultimately may provide a mechanism for more targeted therapies in the future (4).

1. Overview of Oscillatory Networks

The mammalian nervous system constantly integrates diverse external sensory stimuli and internal states into a coherent experience in order to appropriately determine future behavior. The ability to carry out such complex computational processing requires highly, temporally organized neuronal networks. Oscillatory synchronization offers one potential solution for this temporal organization. By this mechanism, spatially distinct neuronal networks can become temporally linked (or synchronized) by a common oscillation, allowing for retention of previous information to influence downstream events (5). Neuronal oscillators occur at various levels, ranging from oscillations of a single neuron determined by its biophysical properties, to local field potentials

(LFP) determined by the probabilistic, rhythmic spiking of thousands of neurons, to scalp electroencephalogram (EEG) that sums the oscillations of millions of neurons. The fact that neuronal oscillations are conserved throughout mammalian evolution highlights its potential universal and fundamental role in neuronal computational processing (5, 6). The emergence of a neuropsychiatric phenotype with dyssynchronous networks further alludes to the potential importance of this mechanism (7).

A given oscillation can be characterized at least by its frequency, amplitude, and phase, which together help determine the features of a neuronal network. Broadly, oscillations are categorized and named based on the frequencies that can be observed when recording from groups of neurons, and include delta, theta, alpha, beta, and gamma bands. Oscillatory frequency is inversely related to the time delay of axonal conduction, since a neuron cannot be synchronized to a frequency cycle shorter than the time required to electrically and chemically conduct its action potential (5). At the level of neuronal ensembles, therefore, high frequency oscillations (such as gamma, 30-70 Hz) can only synchronize spatially close neuronal populations, as the time to conduct action potentials long-range would be longer than its frequency cycle. In contrast, low frequency oscillations (such as theta, 4-10 Hz) with longer cycle lengths can synchronize more spatially distinct regions, and thus offer the potential to mediate network interactions in distant neuronal populations (8). Further, an oscillatory frequency is also inversely proportional to its power density (9). This property allows for lower frequency oscillations with greater power densities to temporally synchronize and bind together faster, local oscillations (5). This can manifest physically as amplitude modulation of the higher frequency by the lower frequency oscillation, termed phase-amplitude cross-frequency coupling (10). The interaction of distinct frequency bands (e.g., gamma and theta) by this method allows for the emergence of more complex networks that could mediate higher-order cognitive processing (7). Lastly, phase can be defined by the position of a time point on the oscillation. The relationship of a neuronal action potential to the oscillatory phase holds salient information, and provides an additional mechanism for single neurons to participate in larger neural assemblies (11, 12).

The ability to quantify neuronal synchronization is necessary for experimentally analyzing these networks. Although there are numerous signal analysis techniques, two mathematical models,

both derived from correlational analyses, are used in this thesis and will be specifically addressed here. The first mathematical model is coherence, which is a well studied, accepted, and robust technique commonly used in neuronal network analysis (13). Before this technique is applied, the oscillatory signal (collected in the time domain) must undergo fast Fourier transform (FFT) to convert into a frequency domain in which the amplitude and phase of the signal is calculated within discrete frequency bins. To calculate coherence, the similarity of the amplitude and phase between each FFT frequency bin between the two signals of interest (e.g., LFPs recorded from two spatial distinct electrodes) is quantified. For two signals with a constant relative phase within the same frequency bin, the amplitudes will summate increasing the coherence value toward "1". For signals without any phase relationship, the amplitudes will subtract, decreasing the coherence value toward "0". Importantly, coherence provides a useful measure of the similarity between two signals and thus its synchronization, but offers no directional information as to where the oscillation originates (14).

The second mathematical model is partial correlation (15). In this method, two oscillatory signals are correlated along some feature of the signal (e.g., amplitude), while controlling for the influence of a third signal. This allows for statistical removal of a signal within a neural network without requiring *in vivo* lesioning/inactivation of the actual neural substrate producing the signal. To perform partial correlation analysis, as used in this thesis, the three signals of interest undergo FFT (as described previously) to quantify the power spectrum density (amplitude) into discrete frequency bins; partial correlation of power spectrum density of two signals is performed with removal of the influence of the third signal. This partial correlation can then be compared to the traditional correlation (in which the effect of a third signal is not controlled). If the partial correlation is significantly smaller than the traditional correlation, it suggests the third signal participates in the synchronization between the two signals of interest. Again, this technique quantifies synchronization between oscillatory signals without informing the origin of the oscillation.

2. Impaired Neuronal Oscillations in Schizophrenia

Schizophrenia is a devastating psychiatric disorder that affects over 26 million people globally, and is ranked as the sixth leading global cause of years lost to disability by the World Health Organization (16). Symptoms of schizophrenia can be broadly divided into positive (e.g.,

delusions and hallucinations), negative (e.g., anhedonia), and cognitive (e.g., memory deficits, impaired decision making) categories. These positive symptoms significantly respond to dopamine transmission blockade with antipsychotics. Such pharmacologic responses have resulted in the dopamine hypothesis in which the pathophysiology of schizophrenia is thought to arise from excess dopamine signaling in the mesolimbic area (17). However, dopamine blockade minimally affects the cognitive and negative symptoms, suggesting that the pathophysiology behind these features may arise due to another mechanism. Although positive symptoms tend to be the most striking feature, cognitive deficits serve as the best predictor of long-term functional outcomes, and therefore an understanding of its neural basis is of great importance (18).

Accumulating evidence suggests that the cognitive deficits of schizophrenia, and neuropsychiatric conditions more generally, arise from dysfunctional neuronal networks (19). The majority of work to date has focused specifically on dysfunctional gamma synchrony. Gamma oscillations are high frequency signals that are found in essentially all brain structures. They have been implicated in diverse functions, including perceptual binding of sensory information (6), selective attention (20), and learning and memory (21). Animal models and patients with schizophrenia demonstrate reduced stimulus-evoked gamma band responses and elevated baseline gamma oscillations noise—findings that are likely secondary to impaired glutamatergic and GABA signaling. This impaired gamma synchronization points to one potential neural mechanism for the cognitive deficits found in schizophrenia (17, 22).

Despite gamma oscillatory dysfunction dominating schizophrenia research, evidence suggests that low frequency theta synchronization, specifically between HC and PFC, is also impaired (1, 3, 7). Although understudied in relationship to schizophrenia, theta is one of the most well characterized brain rhythms: it is the defining oscillation in the hippocampus (HC) during REM sleep, and present during wake exploratory behavior (23). HC theta oscillations serve important roles in memory formation, storage, and retrieval (24, 25), and in synaptic plasticity (26, 27). Theta generators originate from the medial septal nucleus (and other extrahippocamal regions), and lesions here eliminate HC theta with resultant impairments in spatial tasks, further highlighting the importance of theta oscillations (24, 28-30).

In contrast to high frequency gamma oscillations that are spatially limited due to conduction delays, theta oscillations can temporally coordinate local neuronal ensembles over large distances (5). Limited evidence in animal models and humans suggests that impaired long-range coordination between neuronal networks may underlie some of the cognitive deficits observed in schizophrenia. For example, genetic schizophrenic mouse models with a 22q11.2 microdeletion demonstrate decreased theta synchronization between the HC and PFC, and decreased phase locking of PFC neurons to HC theta (3). In schizophrenic rat models in which synthetic immune system activator polyriboinosinic-polyribocytidylic acid is injected into pregnant dams, rat offspring have decreased theta HC-PFC synchronization that correlates with schizotypal behavior measures (decreased prepulse inhibition of startle); these rats also show reduced firing of theta-modulated, gamma-entrained PFC neurons (1). Patients with schizophrenia also demonstrate impaired long-range communication between HC and PFC (31). In a study of monozygotic twins discordant for schizophrenia, affected twins had smaller HC volume and decreased regional blood flow to PFC during the Wisconsin Card Sorting task (32). Patients with schizophrenia also show abnormal connectivity between HC and PFC, as demonstrated by PET (33) and fMRI (34) imaging modalities.

3. The Prefrontal Cortex and Hippocampal Circuitry

As indicated previously, temporal coordination of PFC and HC neuronal ensembles serves an important role in cognition, and disruption of this network contributes to the pathophysiology of schizophrenia. Therefore, a better understanding of pathways involved in HC-PFC coupling will likely offer insight into this illness.

HC-to-PFC Theta Synchronization

Based on anatomical and electrophysiological studies, CA1 and subiculum of HC exhibit a monosynaptic, unidirectional projection to the pyramidal cells in layers II-VI of prelimibic and infralimibic regions of mPFC (35-38). These projections use an excitatory neurotransmitter (likely glutamate) that can be activated by pharmacologic administration of AMPA and NMDA agonists. This early monosynaptic excitation can be followed by inhibitory postsynaptic potentials, likely due to activation of local GABAergic interneurons (37, 39). (See Fig. 7A for anatomical model of HC-PFC connections). Functionally, HC can communicate with PFC neuronal populations by synchronizing PFC neurons to HC theta oscillations. HC-PFC theta

coupling occurs during various memory tasks, and performance in these tasks correlate to the degree of synchronization (2, 28, 40). Further, PFC neurons fire consistently within 100ms after HC neurons in naturally sleeping animals (41), and mPFC neurons phase-lock best to HC theta rhythms delayed by ~50ms during spatial navigation (42). Electrode recordings in human subjects also demonstrate increased HC-PFC synchronization during memory tasks with a directionality preference from the HC-to-PFC as established by Granger causality analysis (43). EEG also records frontal theta oscillations in humans during memory tasks (44). Together, these studies provide strong evidence for functional HC-to-PFC interactions driven by theta oscillations.

PFC-to-HC synchronization

Most research investigation to date has focused heavily on HC driving theta oscillations in PFC, which suggests a somewhat passive role of PFC. However, PFC performs complex cognitive roles, including goal-direct behaviors, decision making, working memory, and attention (45, 46), and therefore, must be able to exert "top-down" influence on other brain regions, like HC. This bias towards HC-to-PFC directionality is at least twofold. Firstly, as previously described, the monosynaptic HC-to-PFC projection is well characterized, whereas no direct projection exists from PFC-to-HC, but instead occurs indirectly through multisynaptic connections, such as through nRe (46, 47). Secondly, HC theta is a very well studied brain oscillation (24, 30), but oscillatory features of PFC are less known. This thesis attempts to directly address both these issues, and will be discussed in more detail individually.

Nucleus Reunions: Potential Functional Mediator of PFC-to-HC Projections

Although no known direct, monosynaptic PFC-to-HC projections exist, nRe—the largest of the midline thalamic nuclei—is ideally situated to play a functional role in this network, since it has reciprocal connections with both mPFC and HC. More specially, anatomical anterograde and retrograde tracing studies indicate that nRe has efferent and afferent mPFC projections (48-50). nRe also forms (presumable excitatory) synapses with pyramidal cells of CA1 (48-50); and CA1 and subiculum of HC also send afferent projections to nRe, suggesting bidirectional flow of information between nRe and HC (47).

Limited previous work also points to a potential role of nRe in memory processing. For example, lesions to nRe impair performance in spatial working memory (51). nRe and PFC neurons also exhibit similar "trajectory-dependent firing" (i.e., significant changes in neuronal firing rates depending on the spatial trajectory of the mouse in a maze) as CA1 neurons; and nRe optogenetic silencing reduces trajectory-depending firing in CA1, suggesting that nRe may mediate PFC informational flow to HC (52). Interestingly, inactivation of nRe (either directly or via mPFC inputs) affects performance in fear conditioning tasks, and may have potential implications in the pathophysiology of post-traumatic stress disorder (53). Together, these studies suggest nRe plays a functional role within the previously described anatomical network.

2-5 Hz: Potential Neural Oscillator of PFC

If nRe provides a potential functional anatomical route by which PFC can reciprocally influence HC activity, by what mechanism could PFC exert its influence on HC? Given the spatial distance between PFC and HC, a low frequency oscillation (distinct from theta) that temporally coordinates HC activity is a likely candidate.

More recently, Fujisawa and Buzsaki (2011) proposed a mechanism by which HC-PFC coupling could involve a second, narrow, spectral peaked oscillation (2-5 Hz) within the delta band. In a maze task, this 2-5 Hz oscillation was the dominant PFC signal, and 2-5 Hz oscillatory power increased during key decision points in the maze, suggesting its potential role in working memory. As previously described, these authors found that theta was the dominant oscillation in HC. Together, the 2-5 Hz and theta oscillations modulated PFC gamma oscillations and neuronal action potentials (54). This study provides preliminary evidence of two distinct low frequency oscillations (2-5 Hz and theta) that can temporally organize local gamma oscillations in PFC. More broadly, the interaction of 2-5 Hz and theta oscillations offer a potential mechanistic framework as to how PFC and HC can reciprocally exert influences on each other. Fujisawa and Buzsaki (2011) also nicely summarize that this 2-5 Hz oscillation has been recorded (but not emphasized) in previously published studies in rats during exploration (55, 56) and under urethane anesthesia (57, 58), suggesting that this 2-5 Hz oscillation is likely ubiquitous.

4. Specific Aims

This thesis proposes a novel thalamocortical neural network by which bidirectional PFC and HC coupling occurs. **Our overall hypothesis is that synchronization from HC-to-PFC direction**

is mediated by HC theta oscillations, and synchronization from PFC-to-HC direction occurs via a 2-5Hz oscillation, which is mediated through the thalamic nRe. This hypothesis was tested through two specific aims:

Aim 1: To characterize HC theta and PFC 2-5 Hz oscillations during pontine reticular formation (RPO) stimulation in urethane-anesthetized rats, and determine whether HC-PFC synchronization occurs though these two oscillations. Fujisawa and Buzsaki (2011) previously described how PFC 2-5 Hz and HC theta oscillations together can co-modulated PFC gamma oscillations in freely moving rats during spatial tasks (54). However, the relationship between these two oscillations has not been characterized in further studies, including characterization in more controlled experimental settings with urethane-anesthetized rats. HC theta oscillations have been well described in urethane-anesthetized rats, and occur under at least two conditions: 1) theta that occurs spontaneously around 4-Hz, and alternates with wide-band delta (59); 2) theta that is induced via RPO stimulation in which the entire theta range (4-10 Hz) can be achieved (60-63). A reliable linear correlation exists between RPO stimulus intensity, and theta frequency and amplitude; this provides a satisfactory experimental model to induce and to study the effects of theta in the rat brain (64, 65). In contrast, although PFC 2-5 Hz oscillations have been previously described in urethane-anesthetized rats (57, 58), this signal has not been characterized during HC theta induction by RPO stimulation. For Aim 1, we characterized HC-PFC synchronization at both the 2-5 Hz and theta oscillation during RPO theta induction in urethane-anesthetized rats.

Aim 2: To establish whether nRe functionally participates in PFC-HC coupling. Unlike the monosynaptic, HC-to-PFC coupling mediated by HC theta drive (37, 38, 43, 66), PFC projects back to HC indirectly through nRe (49, 67). Based on anatomical tracing studies, nRe is ideally located to mediate coupling in PFC-to-HC direction (48, 67), and we hypothesized that this coupling occurs via a distinct 2-5 Hz oscillation. To test this hypothesis, in Aim 2, nRe influence was removed either statically (using partial correlations) or experimentally (by *in vivo* pharmacologic inactivation with lidocaine). Then, theta and 2-5 Hz oscillatory synchronization between PFC and HC was quantified before and after nRe removal. Both statistical and experimental methods were used for nRe removal, due to unique limitations of each: while

partial correlation is a theoretical model that can precisely remove the statistically influence of a signal, it can only predict *in vivo* results. In comparison, while lidocaine injection is an *in vivo* technique and therefore more generalizable, it is an imprecise experimental method to inactive a local region, and off-target effects cannot be completely controlled. The convergence of result by two separate methods will therefore provide more compelling evidence of nRe influence.

Methods

1. Animals

15 male Sprague-Dawley rats (300-550 g, Charles River Laboratories in Massachusetts, USA) were used in this study. The procedures described were conducted in accordance with the Institutional Animal Care and Use Committee of Harvard Medical School and Beth Israel Deaconess Medical Center (Boston, MA, USA).

2. Surgical Procedures

All animals were anesthetized using urethane (1.2-1.5 g/kg of 65-80% solution, intraperitoneal injections). Urethane anesthesia was selected to allow for induction of theta oscillations in HC through stimulation of RPO, as described previously (29, 59, 63). The head of the animal was fastened in a stereotaxic frame, and small burr holes were made to allow for microelectrode placement. Two pairs of twisted stainless steel wires with 1mm distal separation were implanted in dHC corresponding to dentate gyrus and CA1 (3.7 mm posterior to bregma, 2.2 mm lateral to midline, and 4.8 mm below the brain surface), and in nRe (2.5 mm posterior to bregma, on the midline, and 6.5 mm below the brain surface). Two single microelectrode wires were implanted in the right and left prelimbic PFC (3.2 mm anterior to bregma, ± 0.5 mm lateral to midline, and 4.8 mm below the brain surface). A pair of stimulating stainless steel microelectrodes was implanted in RPO (8 mm posterior to bregma, 1.5 mm lateral to midline, and 8 mm below the brain surface). Skull screws overlying the nasal bone and cerebellum served as the reference and ground electrodes, respectively. Electrode wires and screws were secured with dental cement. Microelectrodes were connected to an amplifier (A-M systems), and RPO stimulating electrodes were connected to the stimulation apparatus Master-8 (A.M.P.A).

3. Electrophysiological Recordings

HC theta rhythm was elicited by electrical stimulation of RPO (0.1 ms square waves at 100 Hz for a duration of 10 s). Series of various stimulation intensities (range 0.1 mA-1mA) were applied to find 1) the minimum intensity that produces HC theta rhythm; and 2) the maximal intensity after which theta frequency and/or amplitude did not increase with further increases in current level *(60, 61)*. Once this range was obtained, five levels of stimulus intensity of equal interval that spanned this range were determined. For each trial, each of these five levels of stimuli intensity were then applied individually for 10 s in random order with >60 s seperation

between stimuli. LFPs were recorded using DASYlab 7.0 Acquisition System Laboratory (National Instruments).

4. Pharmacological Inactivation of the Thalamic Nucleus Reuniens

In 4 rats, a guided cannula was implanted in nRe. Three pairs of recording electrodes were implanted: 1) a microelectrode in the left and right prelimbic PFC, respectively (3.2 mm anterior to bregma, ± 0.5 mm lateral to midline, and 4.8 mm below the brain surface); 2) twisted stainless steel wires with 1mm distal separation in dHC to record from dentate gyrus and CA1 (3.7 mm posterior to bregma, 2.2 mm lateral to midline, and 4.8 mm below the brain surface); 3) twisted stainless steel wires with 1mm distal separation in vHC. Stimulating electrodes were implanted in RPO, as described previously. Before lidocaine injection, control recordings were performed during RPO stimulation using previously described protocol. After control recordings, lidocaine (0.2 mg/microliter, volume of 1 microliter) was microinfused using a syringe pump at a rate of 347 nanoliters/min. After lidocaine infusion, theta was elicited through RPO stimulation and electrophysiological recordings were performed as described previously.

5. Histological Procedure

After experiment completion, rats were deeply anesthetized, and brains were removed and fixed in formalin for at least one week. The brains were then transferred to 20% sucrose solution for 24-hours before sectioning with the freezing microtome (Microm HM 450, Thermo Scientific) for cryoprotection during rapid freezing. The brains were mounted on the microtome platform with Tissue-Tek® and frozen with dry ice. Brains were sectioned at 50 microns in the coronal plane. Sections were stored in 20% phosphate-buffered saline with sodium azide, and then mounted on Superfrost plus microscope slides (Fisher Scientific) using a gelatin buffer. Sections were stained with the Nissl method protocol (Cresyl violet staining), and preserved with a cover slip. Slides were examined under microscopy to confirm electrode placement. The locations of PFC electrodes were verified in the prelimbic cortex. HC electrodes were verified in, above, and below the HC fissure. nRe electrodes were verified within the thalamus midline, within or in the close vicinity of nRe.

6. Data Analysis

Using MATLAB (MathWorks) code created in-house, LFPs from HC, PFC, and nRe microelectrodes during each 10 s RPO stimulation were extracted from DASYlab 7.0 (National

Instruments). The middle six seconds of the stimulus was selected in order to remove any movement artifact during the initial two seconds after RPO stimulation, and to remove signal from the last two seconds in which theta may no longer be present. After stimulus extraction, the signal was filtered between 1 and 70 Hz and sampled at 256 Hz. Signals underwent FFT to obtain power density spectra for discrete frequency bin widths of ~0.5 Hz.

Frequency bins with greatest power (peak frequencies) were identified in HC and PFC, respectively. In HC, these frequencies were within the theta band; and PFC and nRe power spectra densities were then calculated within this previously identified theta frequency bin for each RPO stimulation event. In PFC, peak frequencies were present within the 2-5 Hz delta band; and HC and nRe power spectra densities were then calculated within this previously identified 2-5 Hz frequency bin for each RPO stimulation event. Spectra were normalized across experiments using the following method: the minimum and maximum of the peak power at any of the two frequencies across all stimulation instances for a given electrode in a given experiment was calculated; power values were then corrected by subtracting the minimum and dividing by the range to obtain values between 0 and 1.

To examine how RPO stimulation affected the frequency of HC theta and PFC 2-5 Hz oscillations, linear regression (Pearson's correlation) analysis was performed between RPO stimulus intensity and previously identified peak frequencies during each RPO stimulation trial for HC theta and PFC 2-5 Hz oscillations, respectively. To examine how RPO stimulation affected the amplitude (power) of HC theta oscillation in HC, PFC, and nRe, linear regression analysis (Pearson's correlation) was calculated between RPO stimulus intensity and HC, PFC, and nRe power, respectively, within the previously identified peak HC theta frequency bins. This latter analysis was repeated for PFC 2-5 Hz oscillation to determine how RPO stimulation affected power of PFC 2-5 Hz in the HC, PFC, and nRe.

To determine synchronization of theta and 2-5 Hz oscillations among PFC, HC, and nRe, Pearson's correlations were calculated between power densities. To analyze theta synchronization, PFC, HC, and nRe power spectra obtained from the previously identified peak HC theta frequency bin were used to calculate three pairwise correlations between PFC-HC,

PFC-nRe, and HC-nRe. To analyze 2-5 Hz synchronization across brain structures, this analysis was repeated for the PFC, HC, and nRe power spectra obtained from the previously identified peak PFC 2-5 Hz frequency bin.

Partial correlations were next calculated to determine how statistical removal of nRe influenced this network. To determine the effect of nRe removal on theta HC-PFC synchronization, PFC, HC, and nRe power spectra that was obtained from the previously identified peak HC theta frequency bins served as variables for the partial correlation formula below, for which the influence of nRe was controlled. This analysis was repeated for 2-5 Hz oscillations to examine the effect of nRe removal on 2-5 Hz PFC-HC synchronization.

Partial correlation equation for which nRe signal is controlled:

$$r\left(\frac{PFC-HC}{nRe}\right) = \frac{r(PFC-HC)-r(PFC-nRe)*r(HC-nRe)}{\sqrt{(1-r(PFC-nRe)^2)*(1-r(HC-nRe)^2)}}$$

To determine the *in vivo* effect of nRe inactivation, coherence spectra were calculated from rats that underwent local lidocaine nRe inhibition. Coherence spectra between HC and PFC LFPs (before and after lidocaine administration) were calculated for all eight possible pairwise combinations between two PFC (left and right prelimbic area) and four HC (two in dHC, two in vHC) signals for each RPO stimulation trial. Coherence was calculated on overlapping 4 s windows resulting in coherence spectra with 0.5 Hz resolution for each RPO stimulus intensity level. Since 2-5 Hz oscillation power was greatest at low RPO stimulation intensities and theta oscillation power was greatest at high RPO stimulation intensities (see results section), peak HC-PFC coherence values are reported for the lowest stimulus intensity for 2-5 Hz oscillations and the highest RPO stimulation intensity for theta oscillations.

Results are reported as mean ± standard error of the mean, unless specified otherwise.

Results

1. Theta and 2-5 Hz Oscillation Characterization in Urethane-Anesthetized Rats

As described previously (29), HC electrical activity in urethane-anesthetized rats spontaneously alternated between two states:1) large amplitude irregular activity, and 2) regular, narrow spectral peak theta rhythm (Fig. 1A-C). PFC also showed a similar pattern of irregular, wide-band activity that then spontaneous alternated to a dominant rhythm with a narrow-spectral peak around 2 Hz in the delta band (57, 58); this spontaneous switch in PFC to a narrow-spectral peak oscillation co-occurred with HC theta (Fig. 1A-C). Frequently in PFC, a strong ~2 Hz oscillatory component also appeared mixed within the background of irregular delta activity in the "passive" state (i.e., when theta was absent in HC), which is demonstrated by the sharp spectral peak on top of wide-band delta in PFC (Fig. 1D). Spectral analysis of PFC and HC during spontaneous narrow-band oscillations demonstrated that ~2 Hz and theta oscillations co-occurred in both PFC and HC, although ~2 Hz oscillation had greater power in PFC and theta oscillation had greater power in HC (Fig. 1A, 1E). Both oscillations also co-occurred in nRe (Fig. 1A).

Both the appearance of LFP traces and the spectral representation of the rhythmic PFC signal showed essential similarities with HC theta rhythm, and significant difference from wide-band delta activity. Similar to HC theta rhythm, PFC rhythmic signals demonstrate a sharp spectral peak around ~2 Hz. This contrasts from the wide-band delta activity (Fig. 1D), whose spectral properties demonstrate a wide area under the curve for a given "peak" with slow tapering toward higher frequencies (~4 Hz) on one side, while the other side (~0.5 Hz) is limited by the high-pass filter of AC coupled recording. Thus, to avoid confusion of these fundamentally different delta-band activities (narrow band at ~2 Hz versus wide-band delta), we use the term "2-5 Hz oscillations" to denote sinusoidal-like activity within the delta band, which dominated PFC signal in "active" states (i.e., when theta was present in HC).

2. RPO Stimulation Simultaneously Induces 2-5 Hz Oscillation in PFC and Theta Rhythm in HC

Electrical stimulation of RPO resulted in reliable sinusoidal oscillations in PFC, HC, and nRe (Fig. 2B-C). Two prominent and distinct rhythms were observed—theta and 2-5 Hz—and were generally present in all three signals to different degrees, depending on the intensity of RPO

stimulation. Figure 2D-F show a representative example of this described finding: in PFC, at low RPO stimulation intensity (0.15 mA), 2-5 Hz oscillation was the dominant PFC signal, whereas at high RPO stimulation intensity (0.33 mA), theta oscillation was the dominant PFC signal (Fig. 2D). In HC, at low RPO stimulation, theta (6.3 Hz) was the dominant HC signal, and higher RPO stimulation levels resulted in higher theta frequencies (7.8 Hz) with greater power (Fig. 2E). Although present to a smaller degree than theta, 2-5 Hz spectral peak was also observed in HC. Both rhythms were present in nRe at low and high RPO stimulation intensities. However, 2-5 Hz oscillation in nRe had greater power at low RPO stimulation intensities, and theta oscillation had greater power in nRe at high RPO stimulation intensities (Fig. 2F). In addition, the dominant theta oscillation at high RPO stimulus intensity was synchronized at 7.8 Hz in all locations (PFC, HC, nRe; Fig. 2D-F).

Linear regression analysis demonstrated that the frequency of both oscillations systematically changed as RPO stimulations varied (Fig. 3D). As shown in previous studies (60, 61), the peak frequency of HC theta rhythm was between 5.4 Hz ± 0.26 and 7.4 Hz ± 0.24, and increased linearly with increasing RPO stimulus intensity ($r = 0.64$, $p < 0.001$, Fig. 3D). The peak frequency of PFC 2-5 Hz oscillation varied between 2.7 Hz ± 0.19 and 3.7 Hz ± 0.3 within the delta band, and also increased linearly with increasing RPO stimulus intensity ($r = 0.37$, $p = 0.001$; Fig. 3D).

Linear regression analysis also demonstrated that theta and 2-5 Hz oscillation power varied systematically with RPO stimulation intensity (Fig. 3A-C, 3E-F). In HC, theta power increased linearly with increasing RPO stimulus intensity ($r = 0.63$, $p < 0.001$; Fig. 3E). However, there was little effect of RPO stimulus intensity on theta power in PFC ($r = 0.11$, $p = 0.36$; Fig. 3E) or nRe ($r = 0.06$, $p = 0.59$; Fig. 3E), suggesting that PFC and nRe do not participate in generation of RPO-induced theta. Contrary to the behavior of theta power, 2-5 Hz power decreased linearly with increasing stimulus intensity in PFC ($r = -0.60$, $p < 0.001$, Fig. 3F) and in nRe ($r = -0.60$, $p < 0.001$, Fig. 3F). Although the magnitude of 2-5 Hz power was consistently lower in HC (than in PFC or nRe), it still showed a similar negative trend ($r = -0.36$, $p = 0.001$; Fig. 3F). Taken together, HC theta power positively correlated with RPO stimulation level, whereas PFC, HC,

and nRe 2-5 Hz power followed an opposite trend, suggesting a possible negative coupling between the generations of these two rhythms.

3. Differential Contribution of nRe to PFC-HC 2-5 Hz and Theta Coupling

Although 2-5 Hz and theta oscillatory powers were most prominent in PFC and HC, respectively, both oscillations were present in nRe, and showed a parallel RPO stimulation-dependent variation in frequency and power as seen in PFC and HC (Fig. 3). More specifically, nRe 2-5 Hz frequency positively correlated with RPO stimulus intensity, whereas nRe 2-5 Hz power negatively correlated with RPO stimulus intensity (Fig. 3C, 3F), similar to 2-5 Hz signal observed in PFC (Fig. 3A, 3F). Both nRe theta frequency and power increased with increasing RPO stimulus intensity (Fig. 3C, 3E), similar to theta signal observed in HC (Fig. 3B, 3E).

To assess synchronization across regions, pairwise correlations of power were calculated between PFC-nRe, PFC-HC, and HC-nRe for theta and 2-5 Hz oscillations. Three separate correlational analyses were conducted using various partitions of the data. In the first analysis, correlations were performed pooling all stimulation episodes into one analysis (n = 537 in 15 rats; Fig. 4A-B). In the second analysis, correlations were calculated separately for each rat to examine differences across experiments (n = 15 rats; Fig. 4C). In the third analysis, only rats with significant PFC-HC correlations for both theta and 2-5 Hz oscillations (as determined by the second analysis, n=7; Fig. 5A) were selected for partial correlational analysis to examine the statistical effect of nRe signal removal. Rats without significant HC-PFC coupling (n= 8) were excluded from this partial correlational analysis, as examining the effect of nRe removal on HC-PFC coupling on rats in which HC-PFC are not coupled provides interpretable results.

In the first analysis in which all stimulation episodes were pooled, all pairwise correlations were significant ($p < 0.001$) for both theta and 2-5 Hz oscillations. However, correlations for 2-5 Hz were consistently stronger than for theta. The largest correlation overall was between 2-5 Hz PFC-nRe ($r = 0.82$), about 30% larger than the two other 2-5 Hz oscillation pairs ($r = 0.5$ for both PFC-HC and HC-nRe). Similarly, the strongest theta correlation was between nRe and the presumed HC origin of theta rhythm ($r = 0.37$ for HC-nRe vs. $r = 0.2$ for PFC-nRe and HC-PFC).

In the second analysis, pairwise correlations between PFC-nRe, PFC-HC, and HC-nRe were calculated separately for each rat (n = 15) for theta and 2-5 Hz oscillations (Table 1). Significant correlations were found at 2-5 Hz in the majority experiments (i.e., 14/15 rats between PFC-nRE and in 13/15 rats for the other two pairs). Theta correlations between PFC and HC were only significant in 7 out of 15 rats, whereas theta was significant in 11 rats between HC and nRE and in 9 rats between nRE and PFC. Group averages of the second analysis of individual rats (Fig. 4C-D; note that non-significant correlations are shown as r = 0.) paralleled the relationship for correlations of pooled data in the first analysis: 2-5 Hz oscillation power correlations overall were stronger than theta oscillation power correlations, and the largest correlations for either 2-5 Hz or theta was between nRe-PFC and nRe-HC, respectively.

The fact that the strongest correlation for theta oscillations was between nRe-HC (where HC is the presumed origin of theta) and the strongest correlation for 2-5 Hz oscillations was between nRe-PFC (Fig. 4C) suggests that nRe may serve as a relay to establish PFC-HC oscillatory coupling. In the third analysis, only rats with significant PFC-HC correlations at both 2-5 Hz and theta oscillations were selected (n=7; Fig. 5A-B, note larger PFC-HC correlations in this subgroup analysis as compared to whole group analysis in Fig. 4C). Partial correlation analysis was used to calculate the residual PFC-HC correlation after allowance was made for the variations in the rhythmic components of the nRe signal (Fig 5C-E). For 2-5-Hz oscillations, there was a significant decrease in PFC-HC correlation when controlling for nRe (student's paired t-test, $p < 0.001$), from $r = 0.81 \pm 0.03$ (correlation) to $r = 0.13 \pm 0.12$ (partial correlation). This provides evidence that nRe contributes to 2-5-Hz synchrony between the PFC-HC, and removal of this influence almost completely eliminates residual PFC-HC correlation. In contrast, theta PFC-HC correlation ($r = 0.65 \pm 0.07$) and partial correlation ($r = 0.61 \pm 0.08$) were not significantly different (student's paired t-test, $p = 0.53$), suggesting that nRe has minimal effect on theta synchronization between PFC and HC. Partial correlation analysis on the entire population (n=15, data not shown) also consistently showed elimination of PFC-HC 2-5 Hz correlation when controlling for nRe.

Additional comparisons revealed that HC-nRe theta correlation was lower in the sub-group containing only rats with significant theta HC-PFC coupling (r = 0.32, Fig. 5A-B) than whole group analysis with all 15 rats (Fig. 4C). Further, this HC-nRe theta correlation was completely

eliminated when controlling for PFC (partial correlation p(HC-nRe/PFC) = 0.007), indicating that no unique HC-nRe theta coupling existed in these experiments other than that also shared with PFC (Fig. 5E). This may suggest that HC theta drive to nRe occurs through a synapse in the PFC, not via the direct, monosynaptic HC-to-nRe connection. Thus in states where HC and PFC are engaged in theta synchronization, theta flow is largely unidirectional through PFC, despite bidirectional connections between HC and nRe.

4. The effect of nRe *in vivo* Lidocaine Inhibition on PFC-HC Coupling

Lidocaine was microinfused into nRe (n = 4 rats) to pharmacologically inhibit its potential contribution to PFC-HC oscillatory coupling. In these experiments, PFC LFPs were recorded from the left and right prelimibic PFC, and HC field potentials were recorded both in dHC and vHC (two electrodes in each site). Together, this allowed for a total of eight pairwise combinations of PFC-HC recordings in each rat, and coherence was calculated for all pairwise comparisons by RPO stimulus intensity level (Fig. 6A-B). Peak coherence values were identified at low RPO stimulus intensities for 2-5 Hz oscillations, and high RPO stimulus intensities for the theta range (data not shown), likely reflecting the greater spectral power of 2-5 Hz and theta oscillations at low and high RPO stimulation intensities, respectively. Based on these findings, pre- and post-lidocaine coherence comparisons were performed for low RPO stimulus intensities for 2-5 Hz oscillations and high RPO stimulus intensities for theta oscillations. For theta oscillations, lidocaine had little effect on coherence (coherence pre-lidocaine = 0.52 ± 0.04, post-lidocaine = 0.48 ± 0.04, p = 0.19, n=32 from 8 possible pairwise comparisons from 4 rats, Fig. 6C-D), suggesting that nRe does not participate in propagation of theta oscillations between HC and PFC. In contrast, PFC-HC coherence of 2-5 Hz oscillation significantly decreased after lidocaine by 0.39 ± 0.04 (Fig. 6C) from 0.73 ± 0.03 control to 0.34 ± 0.04 after lidocaine ($p < 0.001$, n=32; Fig. 6D). The effect was similar in dHC and vHC (Fig. 6B). These results support the hypothesis that PFC-to-HC 2-5 Hz synchrony is at least partly mediated by nRe, as pharmacologic inactivation of this nucleus significantly decreases coherence between these two brain regions.

Discussion

1. The Role of Theta and 2-5 Hz Oscillation in Bidirectional HC-PFC Synchronization

Electrophysiology recordings performed in urethane-anesthetized rats during RPO stimulation is a well established paradigm that offers the advantage of experimental control over forebrain oscillations without behavioral confines (68). This is the first study (to our knowledge) in which this experimental paradigm was applied to investigate HC and PFC slow oscillations and their relationship. In the resting state without any RPO stimulation, LFPs of both HC and PFC spontaneously alternated between irregular, wide-band activity and a dominant rhythm with a narrow-spectral peak in the delta and/or theta band (57, 58). This spontaneous switch in HC theta has been previously described in urethane-anesthetized rats (29). These two types of delta activity have also been previously described in un-anesthetized animals, depending on different behavioral states. Wide-band delta activity is the well-known dominant EEG pattern of slow wave sleep, whereas highly synchronized neuronal firing generating sinusoidal LFP in PFC was reported in wake rats during working memory task, previously referred to as "4 Hz oscillation" (54).

Importantly, LFP tracings in PFC during RPO stimulation were more similar to HC theta rhythm in several respects, as compared to wide-band delta activity. For one, PFC tracings demonstrated narrow spectral peaks with clear oscillatory properties like theta rhythm. Furthermore, RPO stimulation intensity effectively controlled the frequency and amplitude of both oscillations. Just as the frequency of spontaneous theta rhythm which appears at the lower end (~4 Hz) of the theta band can be increased up to ~7-8 Hz by RPO stimulation (60-62), the frequency of the 2-5 Hz PFC oscillation which spontaneously occurs at ~2 Hz (Kiss et al., 2011a, 2011b) could be increased by RPO stimulation to generate sharp spectral peaks across the entire 2-5 Hz range found in awake rats. However, unlike theta oscillatory power that increased with greater RPO stimulus intensities, the 2-5 Hz PFC oscillatory power demonstrated a negative correlation with RPO stimulation intensities.

In this study, theta oscillations were the dominant frequency in HC during RPO stimulation. Further, peak theta power in HC correlated to PFC power, suggesting HC-PFC theta synchronization that agrees with findings reported in early studies (35-38, 42, 66). Although not

specifically assessed in our study, theta HC-to-PFC synchronization likely plays an important role in learning and memory formation (2, 15, 40, 43, 69). For example, HC-PFC theta coherence in rats peaks during choice points in Y maze tasks, and this coherence is greatest after new rule acquisition (40). Further, electrophysiology recordings in epileptic patients with implanted electrodes demonstrate increased HC-to-PFC theta coherence during recall tasks (43).

HC theta driven PFC synchronization reflects "bottom-up" processing, and has been the primary focus of research to date. However, PFC is theorized to be a master regulator of working memory and higher-order cognitive function (4), yet the mechanism by which PFC exerts "top-down" influences is not clear. A low frequency oscillation that is distinct from HC theta, such as the 2-5 Hz oscillation, may allow for a flexible signal for PFC to synchronize electrical activity with other distant brain regions. As reviewed by Fujisawa and Buzsaki (2011), 2-5 Hz oscillations connecting PFC to other structures may be widespread, as its presence was visible in a number of previous reports even though the authors may not have emphasized them. Besides the presence of this 2-5 Hz oscillation in VTA and HC that was reported by Fujisawa and Buzsaki (2011), 2-5 Hz rhythm of likely PFC origin was present, for example, in striatal recordings (55, 56). Further, 2 and 4 Hz sharp narrow-band coherence with frontal cortical EEG was reported as far as in brainstem sympathetic circuits (70).

The interaction between HC theta and PFC 2-5 Hz band oscillation could therefore provide a flexible network for bidirectional HC-PFC coupling. One potential mechanism for this interaction is through 2-5 Hz-theta oscillation phase coupling by which the 2-5Hz oscillation aligns with the phase of theta by "skipping" every other theta cycle (54, 71, 72). 2-5 Hz-theta phase coupled signals can then modulate both PFC gamma oscillation and individual neuronal spikes in PFC and HC (54). In our study, evidence of theta and 2-5 Hz oscillation interactions were demonstrated based on RPO stimulus intensity level. Specifically, the amplitude of theta and 2-5 Hz signal were negatively coupled: with increasing RPO stimulation, HC theta power increased, whereas PFC 2-5 Hz power decreased. Further evidence of this interaction can be seen when looking specifically at the PFC signals (Fig. 2D): 2-5 Hz oscillation dominated at low RPO stimulus intensities, but theta dominated PFC signals at higher RPO stimulus intensities (although 2-5 Hz oscillation was still present). It is well established that increasing RPO

stimulation levels increase theta amplitude and frequency within HC (60-63). Therefore, with increasing RPO stimulation and thus increased hippocampal theta power generation, HC-to-PFC circuit may dominant, suppressing PFC-to-HC flow. However, when theta drive is minimal (low RPO stimulation intensities) theta suppression may be reduced and 2-5 Hz PFC oscillations could dominant. Together, this suggests potential bidirectional flow between HC and PFC with one signal, either theta or 2-5 Hz, dominating at a given time, depending on various states, such as level of arousal as determined by RPO.

2. The Role of nRe in PFC-to-HC 2-5 Hz Synchronization

Prior tracing studies demonstrate the possibility of the midline thalamic nRe as a potential candidate for mediating communication from PFC-to-HC (67, 73). Two prior electrophysiology studies also suggest a functional role of nRe in mediating PFC-nRe-HC coupling in spatial working memory (52) and fear conditioning (53), and a lesioning study provides additional evidence of nRe role in spatial tasks (51). Our study agrees with a functional role for nRe in mediating PFC-to-HC synchronization. However, our study is the first (to our knowledge) to suggest that PFC-nRe-HC coupling is occurring through a 2-5 Hz oscillation. This is evidenced by 1) partial correlational analysis revealing that 84% of the correlation between 2-5 Hz HC-PFC power densities could be explained by nRe signal, and 2) lidocaine inactivation of nRe significantly reducing 2-5 Hz PFC-HC coherence. These results, together, suggest that PFC-to-HC 2-5 Hz synchronization is mediated by nRe.

For theta oscillations, in contrast, controlling for nRe influence via partial correlations had minimal effect on HC-PFC theta correlation, and lidocaine *in vivo* nRe inactivation had minimal effect on HC-PFC theta coherence. These results support prior evidence that HC-to-PFC communication occurs through an excitatory, monosynaptic connection that is minimally influenced by nRe (35, 36, 38, 66). Of note, however, residual PFC-nRe theta correlation was present when controlling for HC (data not shown), indicating that HC may not be the only source of theta synchronization in PFC. Besides nRe, several other structures have reciprocal connections with PFC and HC (Fig. 7A), which were not recorded in this study, but might have been the origin of these residual correlations for theta. These other regions include the amygdala (AMY), supramammillary nucleus (SUM), entorhinal cortex (EC), medial septum (MS), and

ventral tegmental area (VTA) (47, 74, 75), and therefore should be considered within this network.

Of note, although this thesis emphasized the directionality of theta oscillation in HC-to-PFC direction, the direction of oscillatory flow is likely state-dependent. Subgroup analysis that separated rats based on whether recordings demonstrated HC-PFC theta synchronization (n =7 out of 15) showed smaller HC-nRe theta correlation compared to rats not engaged in HC-PFC synchronization (n= 8 out of 15), such that HC-nRe theta flow decreased during HC-PFC theta synchronization. Further, partial correlation analysis of this subgroup engaged in PFC-HC theta coupling showed that controlling for PFC entirely suppressed nRe-HC theta correlation. This provides preliminary evidence that theta predominately flows unidirectionally from HC-to-PFC-to-nRe during HC-PFC theta engagement (as nRe-HC theta correlation was completely explained by PFC signal), and not through direct HC-to-nRe projections. However, when HC and PFC are not engaged in theta coupling, theta may be directed through HC-to-nRe projections via this alternative, direct pathway.

Prior anatomical studies have not been unable to visualize a direct PFC-to-HC projection until recently. Rajasethupathy et al. (2015) provides singular evidence of a functional monosynaptic PFC (dorsal anterior cingulate) to HC (CA3 and CA1) connection with a potential role in retrieval of encoded memories (76). Although present, the direct PFC-to-HC projections were minor compared to the dense, previously well-described PFC-nRe-HC projections. If a direct HC-PFC projection does exist, however, it raises the question as to why a multisynaptic PFC-nRe-HC projection would dominate over the efficiency of monosynaptic projections—and the answer potentially argues for a critical role of nRe within this network. Since the nRe receives significant inputs from arousal centers of the brain, Vertes et al. (2007) hypothesizes that nRe may gate what information reaches HC based on the arousal levels. In this theorized role, the nRe would actually improve efficiency by ensuring that only salient information to which the animal is attended can be encoded long-term, and less useful information will be discarded (67). Additional research is needed to further elucidate the functional role of nRe within this network.

In summary, the inferences for understanding the dynamical network controlling PFC-HC coupling and the role of nRe are summarized in Fig. 7A. The 2-5 Hz oscillation was the dominant frequency in PFC, correlated with 2-5 Hz power in HC, and was diminished by both statistical and pharmacologic removal of nRe influence. In contrast, theta rhythm was the dominant signal in the HC, correlated with theta power in PFC, and this relationship was minimally affected by nRe signal. In summary, although correlational analysis does not test directionality, our results with prior anatomical and electrophysiological studies provide strong evidence that **HC theta-driven PFC synchronization occurs (at least partially) through direct HC-to-PFC projection, whereas PFC-to-HC communication occurs through synchronization of a 2-5 Hz signal, which is mediated by nRe.**

3. Study Limitations and Future Directions

This study is constrained by several major limitations: 1) the experiments were performed under urethane anesthesia, limiting generalizability to wake animals; 2) *in vivo* lidocaine injections likely achieved imperfect nRe inactivation with off-target site effects; and 3) network directionality is inferred from correlational analyses.

Urethane anesthesia paradigms have many practical and experimental advantages, including extended periods of anesthesia with easy administration, allowance for spontaneous and RPO-induced HC theta oscillations, and reduction of unknown variables associated with freely-moving animals (59-63, 77). However, the generalizability of electrical recordings under urethane anesthesia (and anesthesia more generally) to wake animals is not fully clear. Urethane has nonspecific actions on many neurotransmitter-gated ion channels (including GABA, glycine, AMPA, NMDA, and nicotinic-acetylcholine receptors) (78). Urethane also alters thalamic neuronal responses to noxious stimuli (79), and potentially alters other neuronal responses not yet characterized. Therefore, oscillatory characterization of the proposed HC-PFC network is warranted in wake animals with correlation to the findings presented in this thesis.

Previous work in our laboratory had attempted inactivation of nRe using Designer Receptor Exclusively Activated by Designer Drugs (DREADD) delivered on adeno-associated virus (AAV) via stereotaxic-guided injections (data not presented here). Since nRe has significant volume in the rostral-caudal direction (48), however, targeting the entire nucleus with a single

stereotaxic-guided injection was challenging; this challenge was compounded by the fact that few neurons within the target site even incorporated the virus, as confirmed via immunohistochemistry. As a result of these limitations, significant inactivation of nRe was not attained with DREADD. For this reason, lidocaine inactivation, a more nonspecific agent, was attempted for this thesis. Lidocaine exerts its effect though blockade of fast voltage-gated sodium channels to prevent neuronal depolarization and thus action potential generation. Lidocaine micro-pump infusion through an implanted cannula can reversibly prevent signal transduction of a relatively small population of neurons. It offers the benefit of easy administration, rapid onset, and reversibility. However, similar to viral administration of DREADD, lidocaine blockade is dependent on the location of administration. Further, diffusion to off-site targets, including sites that potentially contribute to 2-5 Hz oscillatory signal, cannot be fully avoided, nor confirmed with histology (only histological evidence of injection is canula placement, as lidocaine does not leave a visible histological trace). Ideally, more targeted and verifiable blockade techniques should be attempted in future studies to more definitively confirm *in vivo* nRe inactivation.

The main statistical analyses performed in this study included Pearson's correlations, partial correlations, and coherence calculations. Although these methods are robust and well-validated techniques, they offer only correlational analysis without direct information regarding directionality within the neural network. Based on the analyses conducted here, directionality was inferred from known anatomical connections with implied polarity (i.e., neuronal signals most commonly flow from dendrites to axons). Further, theta oscillation origin from HC was inferred based on the finding of greatest theta power density of within HC signals and from prior studies (41-43). Although the greatest 2-5 Hz oscillatory power occurred in PFC signals, a non-PFC origin of this oscillation could be explained by several alternative models: PFC 2-5 Hz oscillation induction by VTA (54), from nRe (57, 58, 80-82), or through PFC-nRe reciprocal circuitry (Fig. 7B). Our recordings and analysis cannot differentiate between these models, since partial correlation finds unique variance between two variables (i.e., HC-PFC), which is not shared by the third variable (i.e., nRe), but does not provide information as to where the residual variance originates. Signal analysis that specifically allows for directionality calculations and determination of oscillation origin, for example Granger causality analysis, are needed and will likely offer a deeper mechanistic understanding of PFC-HC coupling (83).

Summary

The major findings of this study are that 1) HC-PFC coupling can be established not only by HC theta rhythm but also by a second narrow-band oscillation in the 2-5 Hz range that dominates PFC activity, and 2) the thalamic nRe is essential for PFC-HC coupling by this second, 2-5 Hz rhythm, whereas theta drive may use the direct HC-PFC pathway.

Figure 7B depicts a functional model based on the findings of this study and prior work. This model is likely dynamic with the strength of 2-5 Hz and theta coupling (depicted as arrow thickness) being state dependent. In one state, HC drives PFC theta (red) synchronization through a direct monosynaptic projection. Although not shown here, PFC likely receives theta drive from outside HC as well. Co-occurring with theta synchrony is a distinct 2-5 Hz oscillation (blue), where the origin of this oscillation may occur within the thalamo-cortical (nRe-PFC) network (although other possible origins cannot yet be excluded). This nRe-PFC network drives the 2-5 Hz oscillation in HC through a direct nRe-HC projection. When HC-PFC are engaged in strong theta synchronization, theta flow is likely unidirectional from HC-to-PFC-to-nRe. However, direct theta flow from HC-to-nRe may increase when HC-PFC are not engaged in theta coupling.

Several aspects of this functional model require further investigation. For one, nRe clearly participates in this circuit, as elimination of its influence reduces PFC-HC 2-5 Hz synchronization, but *why does a multisynaptic projection though nRe exists in the first place? What specific functional role does nRe play in this network?* Secondly, *where is the origin of 2-5 Hz oscillation?* Although an origin within the proposed thalamo-cortical (nRe-PFC) circuit is possible, 2-5 Hz oscillation may arise outside this loop, such as within VTA reward circuits, for example. Thirdly, residual PFC-nRe theta correlation was present when controlling for HC, indicating theta drive originates from additional sources outside of HC. *What other regions contribute to theta drive in nRe-PFC network, and how does this affect the network?* Lastly, the strength of correlations in this network is likely dynamic and state-dependent, and requires further characterization. *What are these different states, and how does this dynamicity affect directionality and oscillatory frequencies within the network?* These questions warrant further elucidation, and will likely enhance our understanding of PFC top-down regulation of learning

and memory. Equally important, this understanding may provide mechanistic insight into the pathophysiology of the cognitive deficits that plaque patients with schizophrenia, and ultimately offer a more targeted therapeutic approach in the future.

References

1. Dickerson DD, Wolff AR, Bilkey DK. Abnormal long-range neural synchrony in a maternal immune activation animal model of schizophrenia. The Journal of neuroscience : the official journal of the Society for Neuroscience. 2010;30(37):12424-31. Epub 2010/09/17. doi: 10.1523/jneurosci.3046-10.2010. PubMed PMID: 20844137.

2. Jones MW, Wilson MA. Theta rhythms coordinate hippocampal-prefrontal interactions in a spatial memory task. PLoS biology. 2005;3(12):e402. Epub 2005/11/11. doi: 10.1371/journal.pbio.0030402. PubMed PMID: 16279838; PubMed Central PMCID: PMC1283536.

3. Sigurdsson T, Stark KL, Karayiorgou M, Gogos JA, Gordon JA. Impaired hippocampal-prefrontal synchrony in a genetic mouse model of schizophrenia. Nature. 2010;464(7289):763-7. Epub 2010/04/03. doi: 10.1038/nature08855. PubMed PMID: 20360742; PubMed Central PMCID: PMC2864584.

4. Teffer K, Semendeferi K. Human prefrontal cortex: evolution, development, and pathology. Progress in brain research. 2012;195:191-218. Epub 2012/01/11. doi: 10.1016/b978-0-444-53860-4.00009-x. PubMed PMID: 22230628.

5. Buzsaki G, Draguhn A. Neuronal oscillations in cortical networks. Science (New York, NY). 2004;304(5679):1926-9. Epub 2004/06/26. doi: 10.1126/science.1099745. PubMed PMID: 15218136.

6. Gray CM, Konig P, Engel AK, Singer W. Oscillatory responses in cat visual cortex exhibit inter-columnar synchronization which reflects global stimulus properties. Nature. 1989;338(6213):334-7. Epub 1989/03/23. doi: 10.1038/338334a0. PubMed PMID: 2922061.

7. Dzirasa K, Ramsey AJ, Takahashi DY, Stapleton J, Potes JM, Williams JK, et al. Hyperdopaminergia and NMDA receptor hypofunction disrupt neural phase signaling. The Journal of neuroscience : the official journal of the Society for Neuroscience. 2009;29(25):8215-24. Epub 2009/06/26. doi: 10.1523/jneurosci.1773-09.2009. PubMed PMID: 19553461; PubMed Central PMCID: PMCPMC2731697.

8. Colgin LL. Oscillations and hippocampal-prefrontal synchrony. Current opinion in neurobiology. 2011;21(3):467-74. Epub 2011/05/17. doi: 10.1016/j.conb.2011.04.006. PubMed PMID: 21571522; PubMed Central PMCID: PMCPMC3578407.

9. Freeman WJ, Rogers LJ, Holmes MD, Silbergeld DL. Spatial spectral analysis of human electrocorticograms including the alpha and gamma bands. Journal of neuroscience methods. 2000;95(2):111-21. Epub 2000/04/07. PubMed PMID: 10752481.

10. Lisman J, Buzsaki G. A neural coding scheme formed by the combined function of gamma and theta oscillations. Schizophrenia bulletin. 2008;34(5):974-80. Epub 2008/06/19. doi: 10.1093/schbul/sbn060. PubMed PMID: 18559405; PubMed Central PMCID: PMCPMC2518638.

11. Canolty RT, Knight RT. The functional role of cross-frequency coupling. Trends in cognitive sciences. 2010;14(11):506-15. Epub 2010/10/12. doi: 10.1016/j.tics.2010.09.001. PubMed PMID: 20932795; PubMed Central PMCID: PMCPMC3359652.

12. Dragoi G, Buzsaki G. Temporal encoding of place sequences by hippocampal cell assemblies. Neuron. 2006;50(1):145-57. Epub 2006/04/08. doi: 10.1016/j.neuron.2006.02.023. PubMed PMID: 16600862.

13. Lowet E, Roberts MJ, Bonizzi P, Karel J, De Weerd P. Quantifying Neural Oscillatory Synchronization: A Comparison between Spectral Coherence and Phase-Locking Value Approaches. PloS one. 2016;11(1):e0146443. Epub 2016/01/09. doi: 10.1371/journal.pone.0146443. PubMed PMID: 26745498; PubMed Central PMCID: PMCPMC4706353.

14. Bowyer SM. Coherence a measure of the brain networks: past and present. Neuropsychiatric Electrophysiology. 2016;2(1).

15. O'Neill PK, Gordon JA, Sigurdsson T. Theta oscillations in the medial prefrontal cortex are modulated by spatial working memory and synchronize with the hippocampus through its ventral subregion. The Journal of neuroscience : the official journal of the Society for Neuroscience. 2013;33(35):14211-24. Epub 2013/08/30. doi: 10.1523/jneurosci.2378-13.2013. PubMed PMID: 23986255; PubMed Central PMCID: PMCPMC3756763.

16. Organization WH. The Global Burden of Disease. 2004.

17. Gandal MJ, Edgar JC, Klook K, Siegel SJ. Gamma synchrony: towards a translational biomarker for the treatment-resistant symptoms of schizophrenia. Neuropharmacology. 2012;62(3):1504-18. Epub 2011/02/26. doi: 10.1016/j.neuropharm.2011.02.007. PubMed PMID: 21349276; PubMed Central PMCID: PMCPMC3264822.

18. Green MF, Kern RS, Braff DL, Mintz J. Neurocognitive deficits and functional outcome in schizophrenia: are we measuring the "right stuff"? Schizophrenia bulletin. 2000;26(1):119-36. Epub 2001/02/07. PubMed PMID: 10755673.
19. Uhlhaas PJ, Singer W. Abnormal neural oscillations and synchrony in schizophrenia. Nature reviews Neuroscience. 2010;11(2):100-13. Epub 2010/01/21. doi: 10.1038/nrn2774. PubMed PMID: 20087360.
20. Fries P, Reynolds JH, Rorie AE, Desimone R. Modulation of oscillatory neuronal synchronization by selective visual attention. Science (New York, NY). 2001;291(5508):1560-3. Epub 2001/02/27. doi: 10.1126/science.291.5508.1560. PubMed PMID: 11222864.
21. Miltner WH, Braun C, Arnold M, Witte H, Taub E. Coherence of gamma-band EEG activity as a basis for associative learning. Nature. 1999;397(6718):434-6. Epub 1999/02/16. doi: 10.1038/17126. PubMed PMID: 9989409.
22. Gonzalez-Burgos G, Lewis DA. GABA neurons and the mechanisms of network oscillations: implications for understanding cortical dysfunction in schizophrenia. Schizophrenia bulletin. 2008;34(5):944-61. Epub 2008/07/01. doi: 10.1093/schbul/sbn070. PubMed PMID: 18586694; PubMed Central PMCID: PMCPMC2518635.
23. Buzsaki G, Rappelsberger P, Kellenyi L. Depth profiles of hippocampal rhythmic slow activity ('theta rhythm') depend on behaviour. Electroencephalography and clinical neurophysiology. 1985;61(1):77-88. Epub 1985/07/01. PubMed PMID: 2408867.
24. Buzsaki G. Theta oscillations in the hippocampus. Neuron. 2002;33(3):325-40. Epub 2002/02/08. PubMed PMID: 11832222.
25. Vertes RP. Hippocampal theta rhythm: a tag for short-term memory. Hippocampus. 2005;15(7):923-35. Epub 2005/09/09. doi: 10.1002/hipo.20118. PubMed PMID: 16149083.
26. Kahana MJ, Seelig D, Madsen JR. Theta returns. Current opinion in neurobiology. 2001;11(6):739-44. Epub 2001/12/13. PubMed PMID: 11741027.
27. Huerta PT, Lisman JE. Heightened synaptic plasticity of hippocampal CA1 neurons during a cholinergically induced rhythmic state. Nature. 1993;364(6439):723-5. Epub 1993/08/19. doi: 10.1038/364723a0. PubMed PMID: 8355787.
28. Young CK, McNaughton N. Coupling of theta oscillations between anterior and posterior midline cortex and with the hippocampus in freely behaving rats. Cerebral cortex (New York,

NY : 1991). 2009;19(1):24-40. Epub 2008/05/06. doi: 10.1093/cercor/bhn055. PubMed PMID: 18453538.

29. Vertes RP, Kocsis B. Brainstem-diencephalo-septohippocampal systems controlling the theta rhythm of the hippocampus. Neuroscience. 1997;81(4):893-926. Epub 1997/10/23. PubMed PMID: 9330355.

30. Winson J. Loss of hippocampal theta rhythm results in spatial memory deficit in the rat. Science (New York, NY). 1978;201(4351):160-3. Epub 1978/07/14. PubMed PMID: 663646.

31. Stephan KE, Friston KJ, Frith CD. Dysconnection in schizophrenia: from abnormal synaptic plasticity to failures of self-monitoring. Schizophrenia bulletin. 2009;35(3):509-27. Epub 2009/01/22. doi: 10.1093/schbul/sbn176. PubMed PMID: 19155345; PubMed Central PMCID: PMCPMC2669579.

32. Weinberger DR, Berman KF, Suddath R, Torrey EF. Evidence of dysfunction of a prefrontal-limbic network in schizophrenia: a magnetic resonance imaging and regional cerebral blood flow study of discordant monozygotic twins. The American journal of psychiatry. 1992;149(7):890-7. Epub 1992/07/01. doi: 10.1176/ajp.149.7.890. PubMed PMID: 1609867.

33. Meyer-Lindenberg AS, Olsen RK, Kohn PD, Brown T, Egan MF, Weinberger DR, et al. Regionally specific disturbance of dorsolateral prefrontal-hippocampal functional connectivity in schizophrenia. Archives of general psychiatry. 2005;62(4):379-86. Epub 2005/04/06. doi: 10.1001/archpsyc.62.4.379. PubMed PMID: 15809405.

34. Lawrie SM, Buechel C, Whalley HC, Frith CD, Friston KJ, Johnstone EC. Reduced frontotemporal functional connectivity in schizophrenia associated with auditory hallucinations. Biological psychiatry. 2002;51(12):1008-11. Epub 2002/06/14. PubMed PMID: 12062886.

35. Swanson LW. A direct projection from Ammon's horn to prefrontal cortex in the rat. Brain research. 1981;217(1):150-4. Epub 1981/07/27. PubMed PMID: 7260612.

36. Jay TM, Witter MP. Distribution of hippocampal CA1 and subicular efferents in the prefrontal cortex of the rat studied by means of anterograde transport of Phaseolus vulgaris-leucoagglutinin. The Journal of comparative neurology. 1991;313(4):574-86. Epub 1991/11/22. doi: 10.1002/cne.903130404. PubMed PMID: 1783682.

37. Thierry AM, Gioanni Y, Degenetais E, Glowinski J. Hippocampo-prefrontal cortex pathway: anatomical and electrophysiological characteristics. Hippocampus. 2000;10(4):411-9.

Epub 2000/09/14. doi: 10.1002/1098-1063(2000)10:4<411::aid-hipo7>3.0.co;2-a. PubMed PMID: 10985280.

38. Hoover WB, Vertes RP. Anatomical analysis of afferent projections to the medial prefrontal cortex in the rat. Brain structure & function. 2007;212(2):149-79. Epub 2007/08/25. doi: 10.1007/s00429-007-0150-4. PubMed PMID: 17717690.

39. Jay TM, Thierry AM, Wiklund L, Glowinski J. Excitatory Amino Acid Pathway from the Hippocampus to the Prefrontal Cortex. Contribution of AMPA Receptors in Hippocampo-prefrontal Cortex Transmission. The European journal of neuroscience. 1992;4(12):1285-95. Epub 1992/01/01. PubMed PMID: 12106392.

40. Benchenane K, Peyrache A, Khamassi M, Tierney PL, Gioanni Y, Battaglia FP, et al. Coherent theta oscillations and reorganization of spike timing in the hippocampal- prefrontal network upon learning. Neuron. 2010;66(6):921-36. Epub 2010/07/14. doi: 10.1016/j.neuron.2010.05.013. PubMed PMID: 20620877.

41. Wierzynski CM, Lubenov EV, Gu M, Siapas AG. State-dependent spike-timing relationships between hippocampal and prefrontal circuits during sleep. Neuron. 2009;61(4):587-96. Epub 2009/03/03. doi: 10.1016/j.neuron.2009.01.011. PubMed PMID: 19249278; PubMed Central PMCID: PMCPMC2701743.

42. Siapas AG, Lubenov EV, Wilson MA. Prefrontal phase locking to hippocampal theta oscillations. Neuron. 2005;46(1):141-51. Epub 2005/04/12. doi: 10.1016/j.neuron.2005.02.028. PubMed PMID: 15820700.

43. Anderson KL, Rajagovindan R, Ghacibeh GA, Meador KJ, Ding M. Theta oscillations mediate interaction between prefrontal cortex and medial temporal lobe in human memory. Cerebral cortex (New York, NY : 1991). 2010;20(7):1604-12. Epub 2009/10/29. doi: 10.1093/cercor/bhp223. PubMed PMID: 19861635.

44. Jensen O, Tesche CD. Frontal theta activity in humans increases with memory load in a working memory task. The European journal of neuroscience. 2002;15(8):1395-9. Epub 2002/05/08. PubMed PMID: 11994134.

45. Miller EK. The prefrontal cortex and cognitive control. Nature reviews Neuroscience. 2000;1(1):59-65. Epub 2001/03/17. doi: 10.1038/35036228. PubMed PMID: 11252769.

46. Vertes RP. Interactions among the medial prefrontal cortex, hippocampus and midline thalamus in emotional and cognitive processing in the rat. Neuroscience. 2006;142(1):1-20. Epub 2006/08/05. doi: 10.1016/j.neuroscience.2006.06.027. PubMed PMID: 16887277.
47. McKenna JT, Vertes RP. Afferent projections to nucleus reuniens of the thalamus. The Journal of comparative neurology. 2004;480(2):115-42. Epub 2004/10/30. doi: 10.1002/cne.20342. PubMed PMID: 15514932.
48. Vertes RP. Analysis of projections from the medial prefrontal cortex to the thalamus in the rat, with emphasis on nucleus reuniens. The Journal of comparative neurology. 2002;442(2):163-87. Epub 2001/12/26. PubMed PMID: 11754169.
49. Herkenham M. The connections of the nucleus reuniens thalami: evidence for a direct thalamo-hippocampal pathway in the rat. The Journal of comparative neurology. 1978;177(4):589-610. Epub 1978/02/15. doi: 10.1002/cne.901770405. PubMed PMID: 624792.
50. Wouterlood FG, Saldana E, Witter MP. Projection from the nucleus reuniens thalami to the hippocampal region: light and electron microscopic tracing study in the rat with the anterograde tracer Phaseolus vulgaris-leucoagglutinin. The Journal of comparative neurology. 1990;296(2):179-203. Epub 1990/06/08. doi: 10.1002/cne.902960202. PubMed PMID: 2358531.
51. Hembrook JR, Mair RG. Lesions of reuniens and rhomboid thalamic nuclei impair radial maze win-shift performance. Hippocampus. 2011;21(8):815-26. Epub 2010/06/24. doi: 10.1002/hipo.20797. PubMed PMID: 20572196; PubMed Central PMCID: PMCPMC2974946.
52. Ito HT, Zhang SJ, Witter MP, Moser EI, Moser MB. A prefrontal-thalamo-hippocampal circuit for goal-directed spatial navigation. Nature. 2015;522(7554):50-5. Epub 2015/05/29. doi: 10.1038/nature14396. PubMed PMID: 26017312.
53. Xu W, Sudhof TC. A neural circuit for memory specificity and generalization. Science (New York, NY). 2013;339(6125):1290-5. Epub 2013/03/16. doi: 10.1126/science.1229534. PubMed PMID: 23493706; PubMed Central PMCID: PMCPMC3651700.
54. Fujisawa S, Buzsaki G. A 4 Hz oscillation adaptively synchronizes prefrontal, VTA, and hippocampal activities. Neuron. 2011;72(1):153-65. Epub 2011/10/11. doi: 10.1016/j.neuron.2011.08.018. PubMed PMID: 21982376; PubMed Central PMCID: PMCPMC3235795.
55. Tort AB, Kramer MA, Thorn C, Gibson DJ, Kubota Y, Graybiel AM, et al. Dynamic cross-frequency couplings of local field potential oscillations in rat striatum and hippocampus

during performance of a T-maze task. Proceedings of the National Academy of Sciences of the United States of America. 2008;105(51):20517-22. Epub 2008/12/17. doi: 10.1073/pnas.0810524105. PubMed PMID: 19074268; PubMed Central PMCID: PMCPMC2629291.

56. Dzirasa K, Coque L, Sidor MM, Kumar S, Dancy EA, Takahashi JS, et al. Lithium ameliorates nucleus accumbens phase-signaling dysfunction in a genetic mouse model of mania. The Journal of neuroscience : the official journal of the Society for Neuroscience. 2010;30(48):16314-23. Epub 2010/12/03. doi: 10.1523/jneurosci.4289-10.2010. PubMed PMID: 21123577; PubMed Central PMCID: PMCPMC3165036.

57. Kiss T, Hoffmann WE, Hajos M. Delta oscillation and short-term plasticity in the rat medial prefrontal cortex: modelling NMDA hypofunction of schizophrenia. The international journal of neuropsychopharmacology / official scientific journal of the Collegium Internationale Neuropsychopharmacologicum (CINP). 2011;14(1):29-42. Epub 2010/03/26. doi: 10.1017/s1461145710000271. PubMed PMID: 20334724.

58. Kiss T, Hoffmann WE, Scott L, Kawabe TT, Milici AJ, Nilsen EA, et al. Role of Thalamic Projection in NMDA Receptor-Induced Disruption of Cortical Slow Oscillation and Short-Term Plasticity. Frontiers in psychiatry. 2011;2:14. Epub 2011/05/11. doi: 10.3389/fpsyt.2011.00014. PubMed PMID: 21556284; PubMed Central PMCID: PMCPMC3089990.

59. Kramis R, Vanderwolf CH, Bland BH. Two types of hippocampal rhythmical slow activity in both the rabbit and the rat: relations to behavior and effects of atropine, diethyl ether, urethane, and pentobarbital. Experimental neurology. 1975;49(1 Pt 1):58-85. Epub 1975/10/01. PubMed PMID: 1183532.

60. Li S, Topchiy I, Kocsis B. The effect of atropine administered in the medial septum or hippocampus on high- and low-frequency theta rhythms in the hippocampus of urethane anesthetized rats. Synapse (New York, NY). 2007;61(6):412-9. Epub 2007/03/21. doi: 10.1002/syn.20388. PubMed PMID: 17372965.

61. Ly S, Pishdari B, Lok LL, Hajos M, Kocsis B. Activation of 5-HT6 receptors modulates sleep-wake activity and hippocampal theta oscillation. ACS chemical neuroscience. 2013;4(1):191-9. Epub 2013/01/22. doi: 10.1021/cn300184t. PubMed PMID: 23336058; PubMed Central PMCID: PMCPMC3547479.

62. McNaughton N, Sedgwick EM. Reticular stimulation and hippocampal theta rhythm in rats: effects of drugs. Neuroscience. 1978;3(7):629-32. Epub 1978/01/01. PubMed PMID: 724111.

63. Vertes RP. An analysis of ascending brain stem systems involved in hippocampal synchronization and desynchronization. Journal of neurophysiology. 1981;46(5):1140-59. Epub 1981/11/01. PubMed PMID: 7299451.

64. Kocsis B, Li S. In vivo contribution of h-channels in the septal pacemaker to theta rhythm generation. The European journal of neuroscience. 2004;20(8):2149-58. Epub 2004/09/29. doi: 10.1111/j.1460-9568.2004.03678.x. PubMed PMID: 15450094.

65. Siok CJ, Rogers JA, Kocsis B, Hajos M. Activation of alpha7 acetylcholine receptors augments stimulation-induced hippocampal theta oscillation. The European journal of neuroscience. 2006;23(2):570-4. Epub 2006/01/20. doi: 10.1111/j.1460-9568.2005.04560.x. PubMed PMID: 16420464.

66. Ferino F, Thierry AM, Glowinski J. Anatomical and electrophysiological evidence for a direct projection from Ammon's horn to the medial prefrontal cortex in the rat. Experimental brain research. 1987;65(2):421-6. Epub 1987/01/01. PubMed PMID: 3556468.

67. Vertes RP, Hoover WB, Szigeti-Buck K, Leranth C. Nucleus reuniens of the midline thalamus: link between the medial prefrontal cortex and the hippocampus. Brain research bulletin. 2007;71(6):601-9. Epub 2007/02/13. doi: 10.1016/j.brainresbull.2006.12.002. PubMed PMID: 17292803.

68. McNaughton N, Kocsis B, Hajos M. Elicited hippocampal theta rhythm: a screen for anxiolytic and procognitive drugs through changes in hippocampal function? Behavioural pharmacology. 2007;18(5-6):329-46. Epub 2007/09/01. doi: 10.1097/FBP.0b013e3282ee82e3. PubMed PMID: 17762505.

69. Hyman JM, Zilli EA, Paley AM, Hasselmo ME. Medial prefrontal cortex cells show dynamic modulation with the hippocampal theta rhythm dependent on behavior. Hippocampus. 2005;15(6):739-49. Epub 2005/07/15. doi: 10.1002/hipo.20106. PubMed PMID: 16015622.

70. Kenney MJ, Gebber GL, Barman SM, Kocsis B. Forebrain rhythm generators influence sympathetic activity in anesthetized cats. The American journal of physiology. 1990;259(3 Pt 2):R572-8. Epub 1990/09/01. PubMed PMID: 2396715.

71. Deshmukh SS, Yoganarasimha D, Voicu H, Knierim JJ. Theta modulation in the medial and the lateral entorhinal cortices. Journal of neurophysiology. 2010;104(2):994-1006. Epub 2010/05/28. doi: 10.1152/jn.01141.2009. PubMed PMID: 20505130; PubMed Central PMCID: PMCPMC2934945.

72. Royer S, Sirota A, Patel J, Buzsaki G. Distinct representations and theta dynamics in dorsal and ventral hippocampus. The Journal of neuroscience : the official journal of the Society for Neuroscience. 2010;30(5):1777-87. Epub 2010/02/05. doi: 10.1523/jneurosci.4681-09.2010. PubMed PMID: 20130187; PubMed Central PMCID: PMCPMC2825159.

73. Varela C, Kumar S, Yang JY, Wilson MA. Anatomical substrates for direct interactions between hippocampus, medial prefrontal cortex, and the thalamic nucleus reuniens. Brain structure & function. 2014;219(3):911-29. Epub 2013/04/11. doi: 10.1007/s00429-013-0543-5. PubMed PMID: 23571778; PubMed Central PMCID: PMCPMC4179252.

74. Cassel JC, Pereira de Vasconcelos A, Loureiro M, Cholvin T, Dalrymple-Alford JC, Vertes RP. The reuniens and rhomboid nuclei: neuroanatomy, electrophysiological characteristics and behavioral implications. Progress in neurobiology. 2013;111:34-52. Epub 2013/09/13. doi: 10.1016/j.pneurobio.2013.08.006. PubMed PMID: 24025745; PubMed Central PMCID: PMCPMC4975011.

75. Dolleman-Van der Weel MJ, Wouterlood FG, Witter MP. Multiple anterograde tracing, combining Phaseolus vulgaris leucoagglutinin with rhodamine- and biotin-conjugated dextran amine. Journal of neuroscience methods. 1994;51(1):9-21. Epub 1994/01/01. PubMed PMID: 7514701.

76. Rajasethupathy P, Sankaran S, Marshel JH, Kim CK, Ferenczi E, Lee SY, et al. Projections from neocortex mediate top-down control of memory retrieval. Nature. 2015;526(7575):653-9. Epub 2015/10/06. doi: 10.1038/nature15389. PubMed PMID: 26436451; PubMed Central PMCID: PMCPMC4825678.

77. Kumar AH, Clover AJ. Intraperitoneal co-administration of low dose urethane with xylazine and ketamine for extended duration of surgical anesthesia in rats. Laboratory animal research. 2015;31(4):174-9. Epub 2016/01/13. doi: 10.5625/lar.2015.31.4.174. PubMed PMID: 26755920; PubMed Central PMCID: PMCPMC4707145.

78. Hara K, Harris RA. The anesthetic mechanism of urethane: the effects on neurotransmitter-gated ion channels. Anesthesia and analgesia. 2002;94(2):313-8, table of contents. Epub 2002/01/29. PubMed PMID: 11812690.
79. Huh Y, Cho J. Urethane anesthesia depresses activities of thalamocortical neurons and alters its response to nociception in terms of dual firing modes. Frontiers in behavioral neuroscience. 2013;7:141. Epub 2013/10/18. doi: 10.3389/fnbeh.2013.00141. PubMed PMID: 24133420; PubMed Central PMCID: PMCPMC3794191.
80. Zhang Y, Yoshida T, Katz DB, Lisman JE. NMDAR antagonist action in thalamus imposes delta oscillations on the hippocampus. Journal of neurophysiology. 2012;107(11):3181-9. Epub 2012/03/17. doi: 10.1152/jn.00072.2012. PubMed PMID: 22423006; PubMed Central PMCID: PMCPMC3378362.
81. Duan AR, Varela C, Zhang Y, Shen Y, Xiong L, Wilson MA, et al. Delta frequency optogenetic stimulation of the thalamic nucleus reuniens is sufficient to produce working memory deficits: relevance to schizophrenia. Biological psychiatry. 2015;77(12):1098-107. Epub 2015/04/22. doi: 10.1016/j.biopsych.2015.01.020. PubMed PMID: 25891221; PubMed Central PMCID: PMCPMC4444380.
82. Nagy D, Stoiljkovic M, Menniti FS, Hajos M. Differential Effects of an NR2B NAM and Ketamine on Synaptic Potentiation and Gamma Synchrony: Relevance to Rapid-Onset Antidepressant Efficacy. Neuropsychopharmacology : official publication of the American College of Neuropsychopharmacology. 2016;41(6):1486-94. Epub 2015/09/26. doi: 10.1038/npp.2015.298. PubMed PMID: 26404843; PubMed Central PMCID: PMCPMC4832008.
83. Kaminski M, Ding M, Truccolo WA, Bressler SL. Evaluating causal relations in neural systems: granger causality, directed transfer function and statistical assessment of significance. Biological cybernetics. 2001;85(2):145-57. Epub 2001/08/18. doi: 10.1007/s004220000235. PubMed PMID: 11508777.

Tables and Figures

Table 1. Percentage of rats (n=15) with significant power density correlations.

	Theta	2-5 Hz
PFC-nRe	9/15 (60%)	14/15 (93%)
PFC-HC	7/15 (47%)	13/15 (87%)
HC-nRe	11/15 (73%)	13/15 (87%)

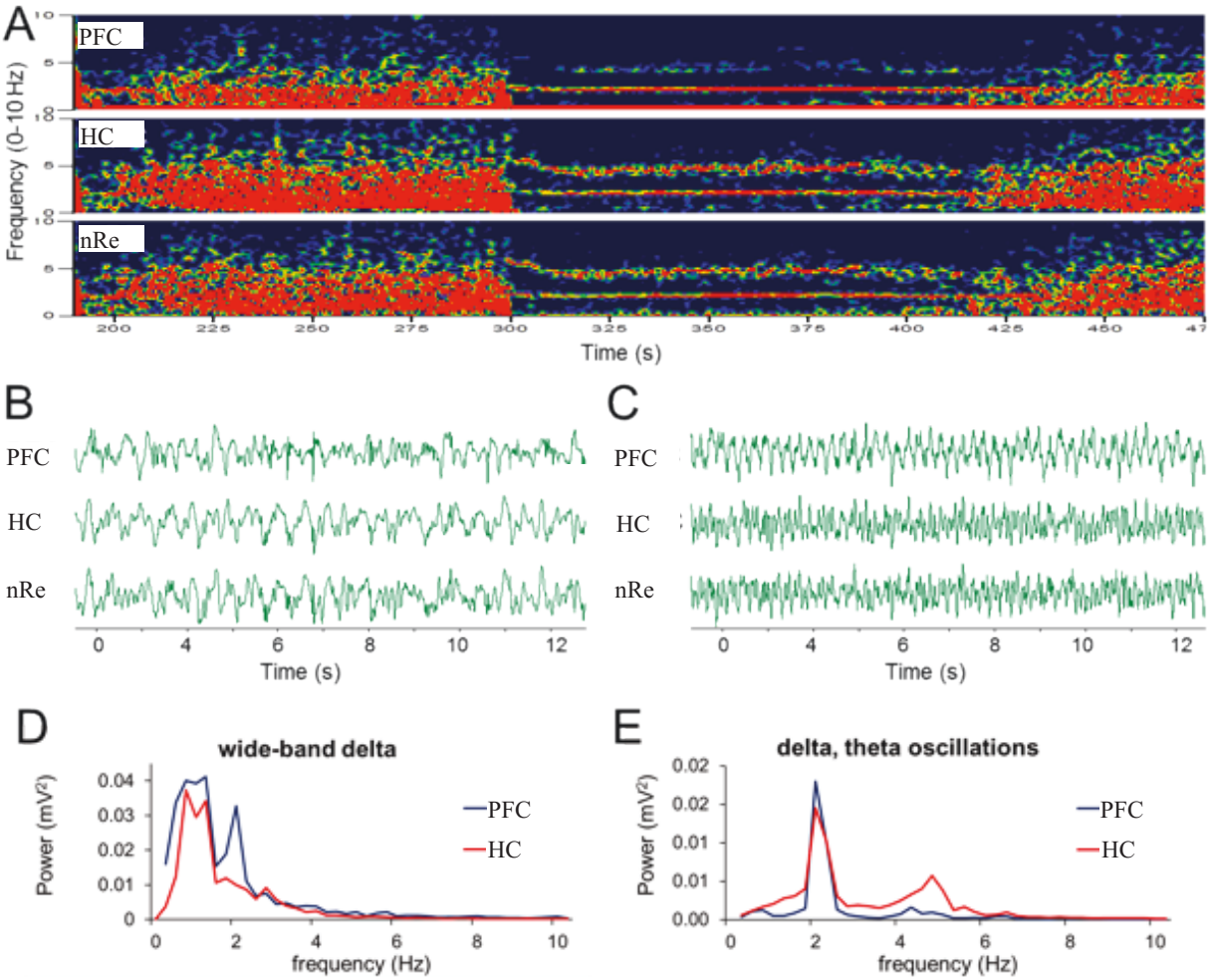

Figure 1. Spontaneous alternation between wide-band delta activity and simultaneous 2-5 Hz and theta oscillations in urethane-anesthetized rats.

A. Examples of time-frequency plots that demonstrate alternations between wide-band delta activity and two oscillations at 1.9 and 4.6 Hz in PFC, HC and nRe. **B-C.** Sample LFP recordings on a faster time scale showing large amplitude irregular activity (B) and rhythmic activity (C). Voltage calibrated to 0.5 mV. **D and E.** Power spectra of 75 s PFC and HC LFP signals exhibiting wide-band spectral components (D) and sharp peaks in the delta and theta band (E). Note that power spectra were overlaid for different signals (HC, PFC) and autoscaled to the largest peak.

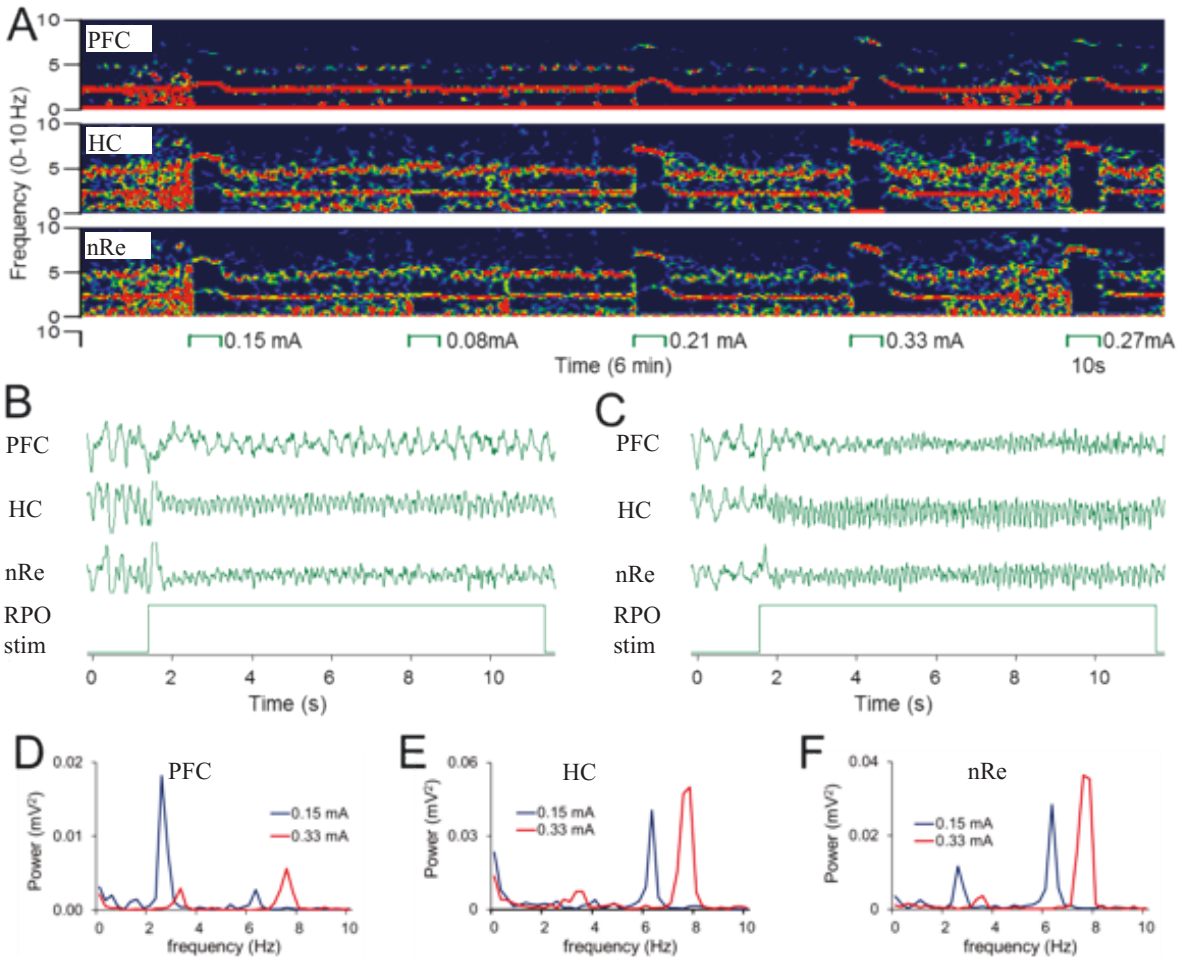

Figure 2. 2-5 Hz oscillation elicited in PFC simultaneously with HC theta by RPO stimulation.

A. Time-frequency plot depicting PFC, HC and nRe oscillations elicited by RPO stimulation at different intensities (between 0.08 and 0.33 mA). **B-C.** Sample LFP recordings that show the induction of PFC 2-5 Hz oscillation and HC theta oscillation with RPO stimulation at low (0.15 mA) intensity (B), and high (0.33 mA) intensity (C). RPO-induced oscillations interrupt ongoing large amplitude irregular waves. Voltage calibrated to 0.5mV. **D-F.** Power spectra of PFC (D), HC (E), and nRe (F) LFP signals shown in B and C during low (blue) and high intensity (red) RPO stimulation.

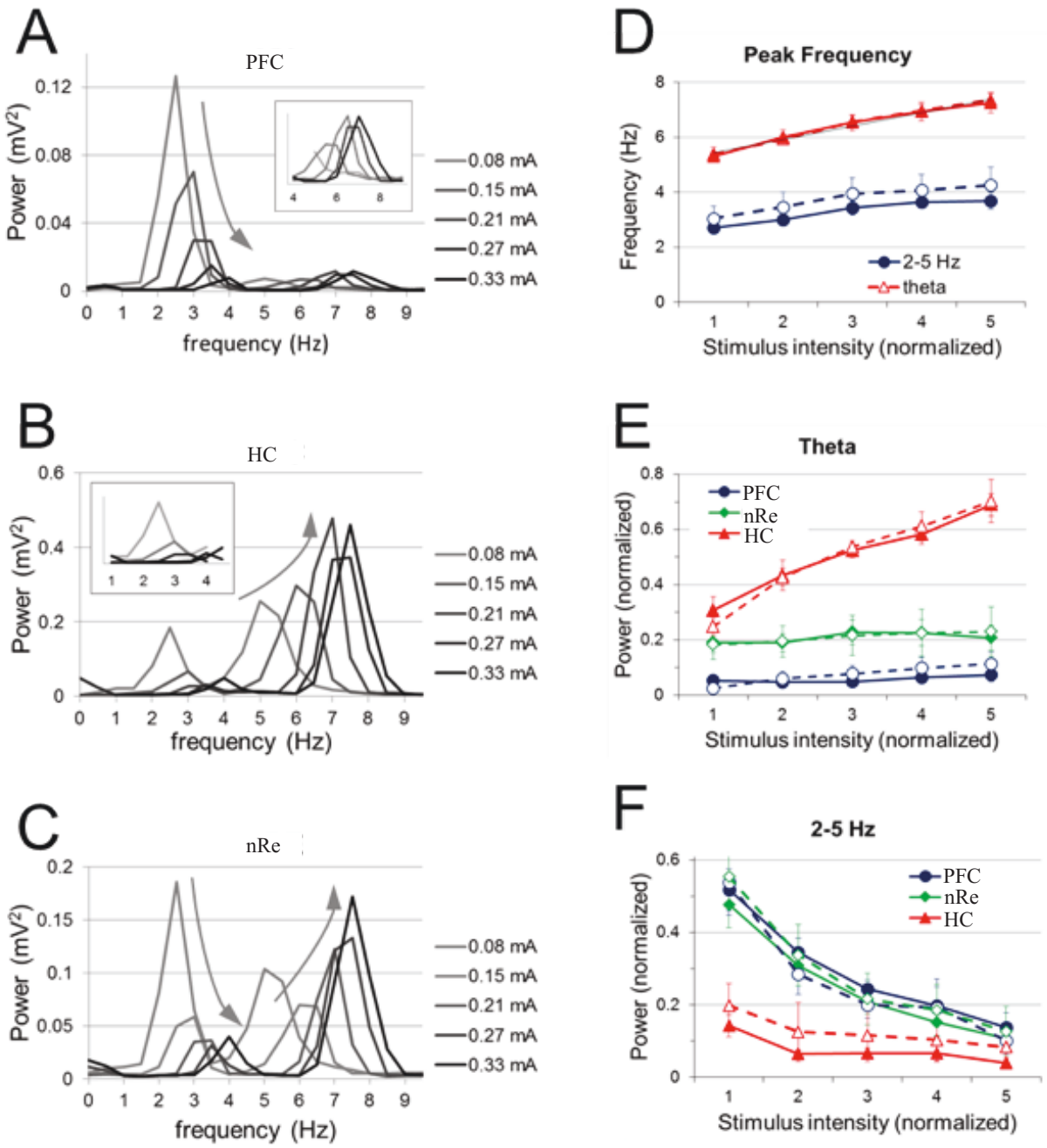

Figure 3. The changes in frequency and power of 2-5 Hz and theta oscillations elicited by stimulation of RPO at five different stimulus intensities.

A-C. Sample power spectra of PFC (A), HC (B), and nRe (C) signals during RPO stimulation at five different intensities. Darker colors and direction of arrow represent increasing stimulus intensities. Inserts in A and B show power spectra in the frequency bands of the non-dominant

components (i.e., 4-9 Hz in PFC and 1-4 Hz in HC) on a larger scale. Note decreasing power but increasing frequency for 2-5 Hz with higher RPO stimulation intensities (A); and increasing frequency and power for theta with higher RPO stimulation intensities (B). **D.** Linear regression analysis for group averages of 2-5 Hz and theta oscillation peak frequencies elicited by RPO stimulation at different intensities. Peak frequency of HC theta oscillation ranged between 5.4 Hz ± 0.26 and 7.4 Hz ± 0.24; Pearson's correlation coefficient, $r = 0.64$, $p < 0.001$. Peak frequency of PFC 2-5 Hz oscillation varied between 2.7 Hz ± 0.19 and 3.7 Hz ± 0.3; Pearson's correlation coefficient, $r = 0.37$, $p = 0.001$. **E-F.** Group averages of spectral power at theta (E) and at 2-5 Hz (F) in PFC, HC, and nRe as a function of RPO stimulation intensity. Peak frequencies for theta and 2-5 Hz were identified on HC and PFC spectra, respectively, and spectral power at these frequencies were averaged for each signal. Linear regression analysis for all rats (n=15) for theta (E) HC: $r = 0.63$, $p < 0.001$; PFC: $r = 0.11$, $p = 0.36$; nRe: $r = 0.06$, $p = 0.59$, and for 2-5 Hz (F) HC: $r = -0.36$, $p = 0.001$; PFC: $r = -0.60$, $p < 0.00$; nRe: $r = -0.60$, $p < 0.001$. In D-F, continuous lines represent averages of all rats (n=15), dashed lines represent experiments with significant PFC-HC correlation (n=7 for theta and n=13 for 2-5 Hz). Error bars represent standard error of the mean.

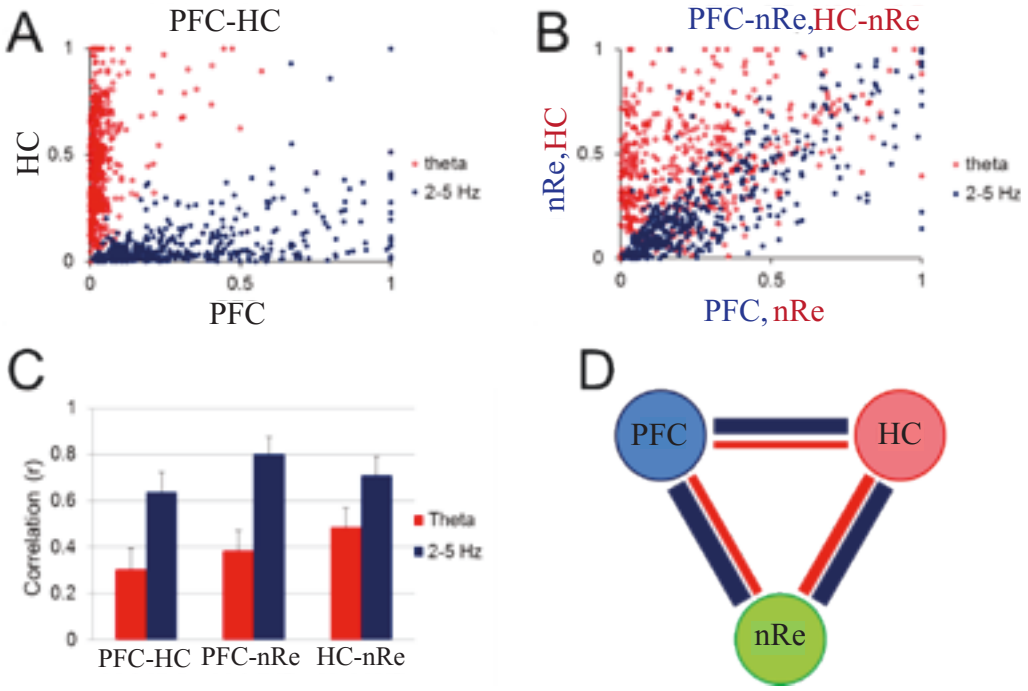

Figure 4. The relationship between PFC, HC, and nRe rhythmic LFPs at 2-5 Hz and theta oscillations.

A. Scatterplot of power between PFC vs. HC at theta (red) and 2-5 Hz (blue) oscillations for all stimulation episodes, n=537 in 15 rats. **B.** Scatterplot of peak power in PFC vs. nRe at 2-5 Hz (blue) and HC vs. nRe at theta (red) oscillations. In A-B, voltages were normalized for each experiment and expressed in arbitrary units between 0 and 1. **C.** Pairwise correlation of 2-5 Hz and theta oscillations between different structures. Correlations were calculated separately for each rat, and average over the group of n=15 rats. All data points were used. Non-significant correlations were set to = 0. Reported as mean ± S.E.M. **D.** Correlation structure of RPO induced oscillations between PFC, HC, and nRe. Thickness of lines is proportional to correlations at 2-5 Hz (blue) and theta (red) frequencies.

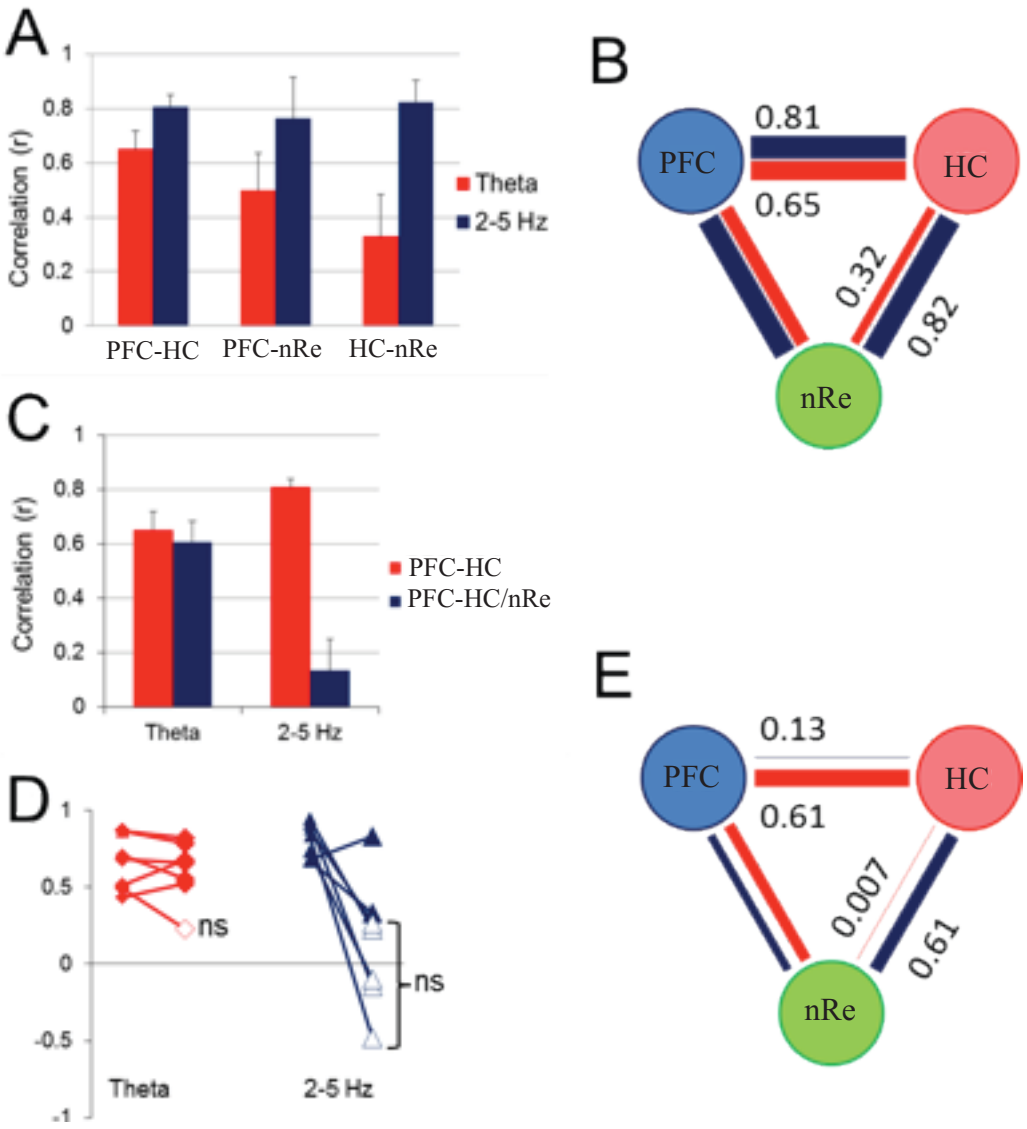

Figure 5. Partialization of significant PFC-HC correlations by nRe.

A. Group averages of power pairwise correlations between PFC, HC, and nRe for 2-5 Hz and theta oscillations. Only experiments with significant PFC-HC correlations at both frequencies were included (n=7). **B.** Correlation structure of RPO induced oscillations between PFC, HC, and nRe for this sub-group. **C-D.** Group averages (n=7) of PFC-HC correlations and PFC-HC/nRe partial correlation (C), and the effect of partialization in individual experiments (D). NS denotes non-significant. **E.** Pairwise partial correlations after controlling for the third signal. Note almost complete elimination of PFC-HC 2-5 Hz correlation (after controlling for nRe

influence), and of HC-nRe theta correlation (after controlling for PFC influence). In B and E thickness of lines is proportional to peak correlations at 2-5 Hz (blue) and theta (red) frequencies.

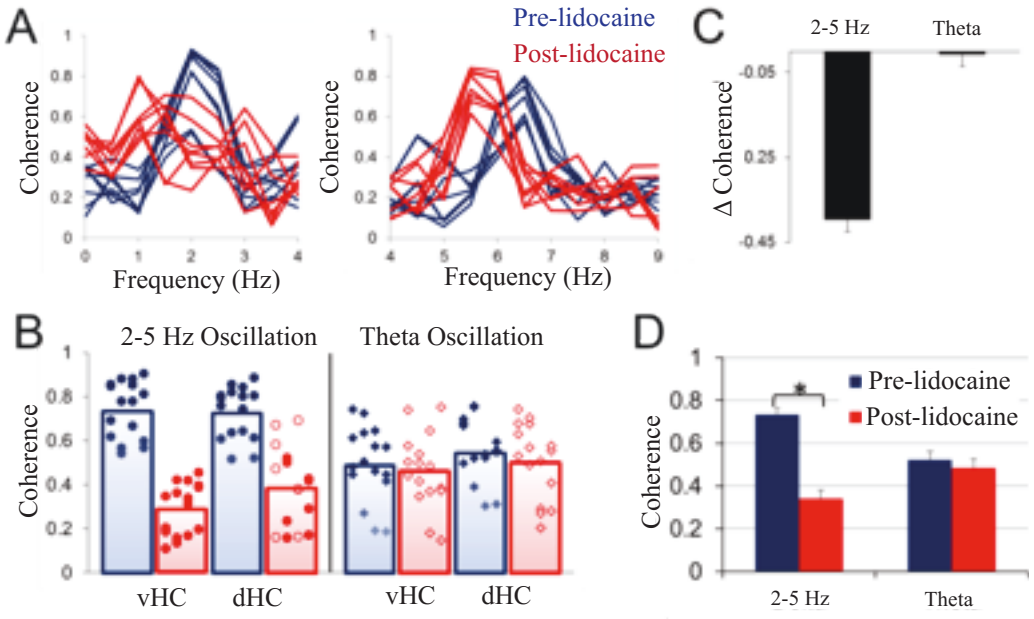

Figure 6. Effect of nRe lidocaine inactivation on HC-PFC 2-5 Hz and theta coherence.

A. Sample HC-PFC coherence spectra from a representative experiment for all pairwise combinations between two PFC and four HC recordings in the delta (0-4 Hz) and theta (4-9 Hz) frequency ranges before (blue) and after (red) microinjection of 0.1 mg lidocaine in nRe, during low (left) and high (right) RPO stimulation. **B.** Pre- (blue) and post-lidocaine (red) peak coherence for pairs of PFC-vHC and PFC-dHC recordings for 2-5 Hz and theta oscillations. Individual peaks are plotted as dots (2-5 Hz) or rhomboids (theta); open symbols mark experiments with no significant drug effect. Each bar represents the mean of peak coherence values for one stimulus intensity for all rats. **C.** The change in peak 2-5 Hz and theta coherence after lidocaine injection, averaged over all PFC-HC pairs (n= 32, 8 PFC-HC combinations in 4 rats). **D**. Group averages of coherence peak values in pre- and post-lidocaine recordings (n= 32). Pharmacological inactivation of the nRe had minimal effect on PFC-HC coherence for theta oscillations ($p = 0.19$), but a significant effect for 2-5 Hz oscillations ($p < 0.001$).

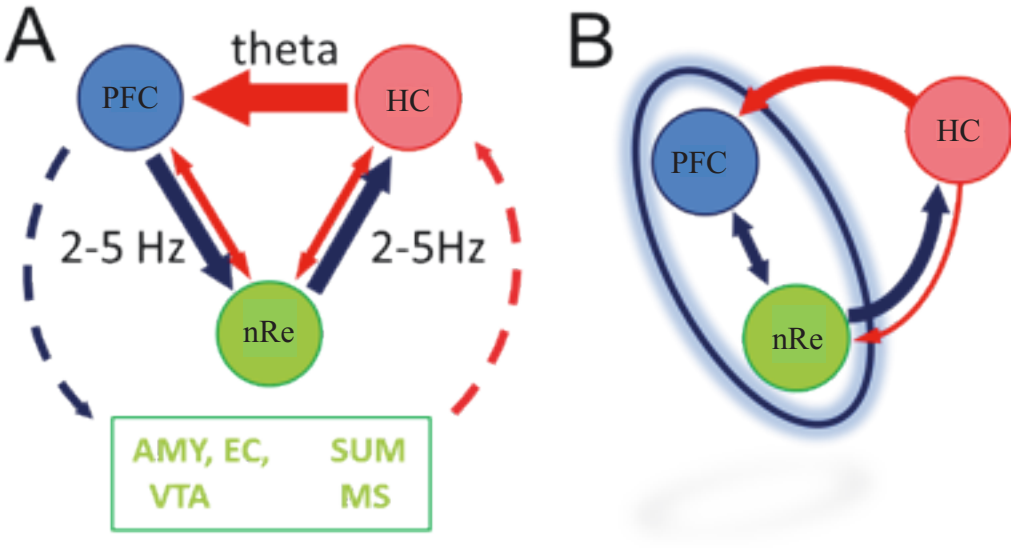

Figure 7. Possible models of HC-PFC oscillatory coupling at two frequencies.

A. Model summarizing the known anatomical connections and their selective involvement (as shown in this study) in conveying 2-5 Hz and theta oscillatory signals between PFC and HC. First, the results presented here are in agreement with the direct HC-to-PFC pathway carrying a theta-synchronizing signal (red). Second, synchronization at 2-5 Hz was found to involve the nRe and could use reciprocal nRe connections with both PFC and HC (blue). Third, several other structures (not recorded in this study) also have reciprocal connections with PFC and HC and could be the origin of residual correlations, including the amygdala (AMY), entorhinal cortex (EC), supramammillary nucleus (SUM), ventral tegmental area (VTA), and medial septum (MS). **B.** Functional model in which 2-5 Hz oscillation is generated by a thalamo-cortical (nRe-PFC) network. PFC is the primary input to this network to receive HC theta influence. The common output of the network to HC is nRe, which utilizes a 2-5 Hz synchronizing signal.